

Recent behavior of the North Anatolian Fault: Insights from an integrated paleoseismological data set

J. Fraser,¹ K. Vanneste,¹ and A. Hubert-Ferrari¹

Received 21 September 2009; revised 23 February 2010; accepted 16 April 2010; published 30 September 2010.

[1] The North Anatolian Fault (NAF) is a right-lateral plate boundary fault that arcs across northern Turkey for ~1500 km. Almost the entire fault progressively ruptured in the 20th century, its cascading style indicating that stress from one fault rupture triggers fault rupture of adjacent segments. Using published paleoseismic investigations, this study integrates all of the existing information about the timing of paleoearthquakes on the NAF. Paleoseismic investigation data are compiled into a database, and for each site a Bayesian, ordering-constrained age model is constructed in a consistent framework. Spatial variability of recurrence intervals suggests a spatial pattern in the behavior of earthquakes on the NAF that may correspond to the tectonic provinces within the Anatolian plate. In the west, the shear stress associated with the escaping Anatolian plate interplays with the tensile stress associated with the Aegean extensional province. Along this western transtensional section we recognize short recurrence intervals and switching between the furcated fault strands. The central section of the NAF is translational with little influence of fault-normal stresses from other tectonic sources. This section tends to rupture in unison or close succession. The eastern section of the NAF is transpressional due to the compressional fault-normal stress associated with the indenting Arabian plate. Along this section the recurrence intervals are bimodal, which we attribute to variable normal stress, although there are other possible causes.

Citation: Fraser, J., K. Vanneste, and A. Hubert-Ferrari (2010), Recent behavior of the North Anatolian Fault: Insights from an integrated paleoseismological data set, *J. Geophys. Res.*, 115, B09316, doi:10.1029/2009JB006982.

1. Introduction

[2] “Like volcanism and changes in sea level, there ought to be broad geological patterns that can help us improve our ability to assess seismic hazard” [Yeats, 2007, p. 863]. One method that may help to illuminate patterns of seismicity in the past is paleoseismology. Paleoseismic investigations determine the approximate timing of surface-rupturing earthquakes using geological and geomorphological evidence along with Quaternary dating methods [e.g., McCalpin, 1996]. But not all surface-rupturing earthquakes are recognized by paleoseismology [Yeats, 2007] and the procedure for considering Quaternary dating data has been evolving over recent decades [e.g., Biasi and Weldon, 1994; Biasi et al., 2002; Hilley and Young, 2008a], which influences how we determine the timing of paleoearthquakes. Therefore, the results from existing paleoseismic investigations have been determined using slightly different methodologies, making it dubious to draw comparisons between them. With a long historical earthquake record [e.g., Ambraseys and Jackson, 1998], a relative abundance of paleoseismic data [e.g., Hartleb et al., 2006; Kozaci, 2008;

Pantosti et al., 2008; Rockwell et al., 2009], and relatively simple fault geometry (i.e., linear without major interacting faults) along the eastern two thirds [e.g., Barka, 1992], the North Anatolian Fault (NAF) is an ideal natural laboratory to study long-term (thousands of years) patterns of seismicity.

[3] The NAF is a ~1500 km long right-lateral strike-slip plate boundary fault that arcs across northern Turkey and accommodates most of the westward translation and clockwise rotation of the Anatolian plate relative to Eurasia [e.g., Barka, 1992; Şengör et al., 2005; Westaway, 2003]. Earthquakes along the NAF have caused destruction to the region throughout history, which is relatively well documented in a long historical record [e.g., Ambraseys and Jackson, 1998]. Most of the NAF ruptured during the 20th century with a spatiotemporal progressive failure pattern that indicates that the rupture of one segment of the fault casts a shadow of increased Coulomb failure stress onto adjacent segments, increasing their probability of failure [Stein et al., 1997]. This tantalizing glimpse of a crustal stress and strain process during a human lifetime is a rare observation in a science where generally we talk of thousands if not millions of years. This highlights two pertinent questions: does the NAF undergo progressive failure during every seismic cycle? And, do earthquakes repeatedly rupture the same (characteristic [e.g., Schwartz

¹Seismology Section, Royal Observatory of Belgium, Brussels, Belgium.

and Coppersmith 1984; Sieh, 1996]) fault segments during each seismic cycle?

[4] The historical earthquake record provides temporally accurate earthquake reports, although data from prior to the 20th century have little spatial precision (i.e., the location and extent of fault rupture is not documented). One of the greatest weaknesses of modern paleoseismic investigation techniques is that they have relatively poor temporal precision owing to the uncertainties associated with Quaternary dating techniques and the relationship between the dated samples and their deposits. However, they do provide spatially precise data (i.e., evidence of an earthquake rupturing a specific point on the fault) and in many cases much longer records of earthquakes. Therefore, by integrating historical and paleoseismological data, we achieve the greatest spatiotemporal understanding of earthquakes, allowing the greatest insight into long-term fault behavior.

[5] In this study, we catalog the existing published paleoseismic data from the NAF using a consistent modern methodology, and analyze the results in light of historical earthquake catalogs. To investigate patterns of seismicity along the NAF, we compare earthquake timing records from existing paleoseismic studies to each other and compare these to the historical earthquake record. In addition to investigating patterns of seismicity we aim to provide a catalog of the existing paleoseismic data from the NAF that can be used to direct further studies on the fault.

2. Seismotectonic Setting of the North Anatolian Fault

2.1. Driving Forces

[6] Figure 1 illustrates that the Anatolian plate is in complex tectonic setting dominated by collision. As the Arabian plate moves north it squeezes the Anatolian plate, which escapes westward in an extrusion like process [Flerit *et al.*, 2004; Şengör *et al.*, 2005]. Additionally, subduction processes at the Hellenic arc cause extension in the western portion of the Anatolian plate, resulting in a westward pulling force on the Anatolian plate and also adding complexity to fault geometry and hence rupture propagation in western sections of the NAF [Flerit *et al.*, 2004; Pondard *et al.*, 2007]. Strain transferred from the moving mantle lithosphere to the crust, throughflow in a weak lower-crustal layer, may exert a dragging force on the Anatolian plate [Westaway, 2003]. Therefore, the Anatolian plate is being pushed, pulled, and dragged from beneath in a westward direction that, over time, results in a westward translation and counter-clockwise rotation of the Anatolian plate, relative to a stable Eurasia. The NAF accommodates almost all of the deformation along the northern edge of the westward moving Anatolian plate, resulting in predominantly right-lateral strike-slip motion. In the west, the NAF gradually diminishes in importance in the Aegean Sea where the dominant tectonic process becomes the aforementioned back-arc extension associated with the Hellenic arc. To the east, the NAF ends near the Kaliova triple junction where, in a complex manner, it meets the East Anatolian Fault, the left-lateral strike-slip fault that accommodates most of the westward movement of the Anatolian plate on its southeast side. The region around the Anatolian plate near the Karliova triple junction is clearly in compression, with much of the

regional shortening occurring in the Caucasus Mountains (Figure 1).

[7] It is possible to divide the Anatolian plate into 3 tectonic provinces, as first proposed by Şengör *et al.* [1985]: the west Anatolian extensional province, the central Anatolian “Ova” province, and the east Anatolian contractional province (Figure 1). Subsequent to the zonation of the Anatolian plate by Şengör *et al.* [1985], paleomagnetic and crustal thickness data has been presented that supports this division. Paleomagnetic directions from paleo- and neotectonic units indicate counter-clockwise rotations in the east Anatolian contractional province [Piper *et al.*, 2008], which we attribute to north–south shortening across the Anatolian plate. Paleomagnetic directions in the central Anatolian Ova province are scattered about a north–south direction [Piper *et al.*, 2008], which we interpret to reflect little deformation since formation. Paleomagnetic directions in the west Anatolian extensional province are rotated clockwise [Piper *et al.*, 2008], which we attribute to rotations associated with extension. The plate thickness in the east Anatolian contractional province is 40–50 km [Zor, 2008], in the central Anatolian Ova province 36–40 km thinning toward the southern edge [Zor, 2008], and in the west Anatolian extensional province spot thicknesses are generally in the range of 22–30 km [Tirel *et al.*, 2004; Zhu *et al.*, 2005], with a thickness of only 8 km in the Sea of Marmara [Bécel *et al.*, 2009]. We assume that the thickness of the plate in the central Anatolian Ova province is approximately that of the whole region prior to the present tectonic regime (i.e., at least 13 Ma.). The thicker crust in the east is interpreted to reflect shortening due to the N–S compressional stress, and the thinner crust in the west is inferred to be due to tensile stress.

[8] Where these tectonic provinces are in contact with the NAF we recognize the (from west to east): western translational, central translational, and eastern transpressional sections of the NAF. We define the eastern boundary of the western Anatolian extensional province by drawing a line between the eastern side of the Hellenic arc and the point where the NAF begins to branch-out or furcate to the west, although this boundary may be farther east [e.g., Allmendinger *et al.*, 2007]. We define the western boundary of the east Anatolian compressional province within the Anatolian plate by drawing a line along the orientation of the western Arabian plate GPS vector [Reilinger *et al.*, 2006] from the intersection of the Dead Sea fault with the East Anatolian fault, which projects to about the Niksar pull-apart basin on the NAF (Figure 1). We are unsure of the nature of the boundaries of these zones; there may be significant transition zones.

2.2. Age and Total Offset

[9] Prior to the formation of the NAF, the geology of the arc along which it now traces was dominated by the Tethyside accretionary complexes, suture zones formed by closing of the Tethys Ocean. As the NAF formed it utilized preexisting weaknesses in the accretionary complexes [Barka, 1992; Şengör *et al.*, 2005]. Because of the preexisting semi-parallel geological structure, defining the total offset and age of the NAF is difficult [Barka, 1992]. Estimates of total offset (Table S1 in the auxiliary material) suggest that the NAF has undergone a right-lateral offset of

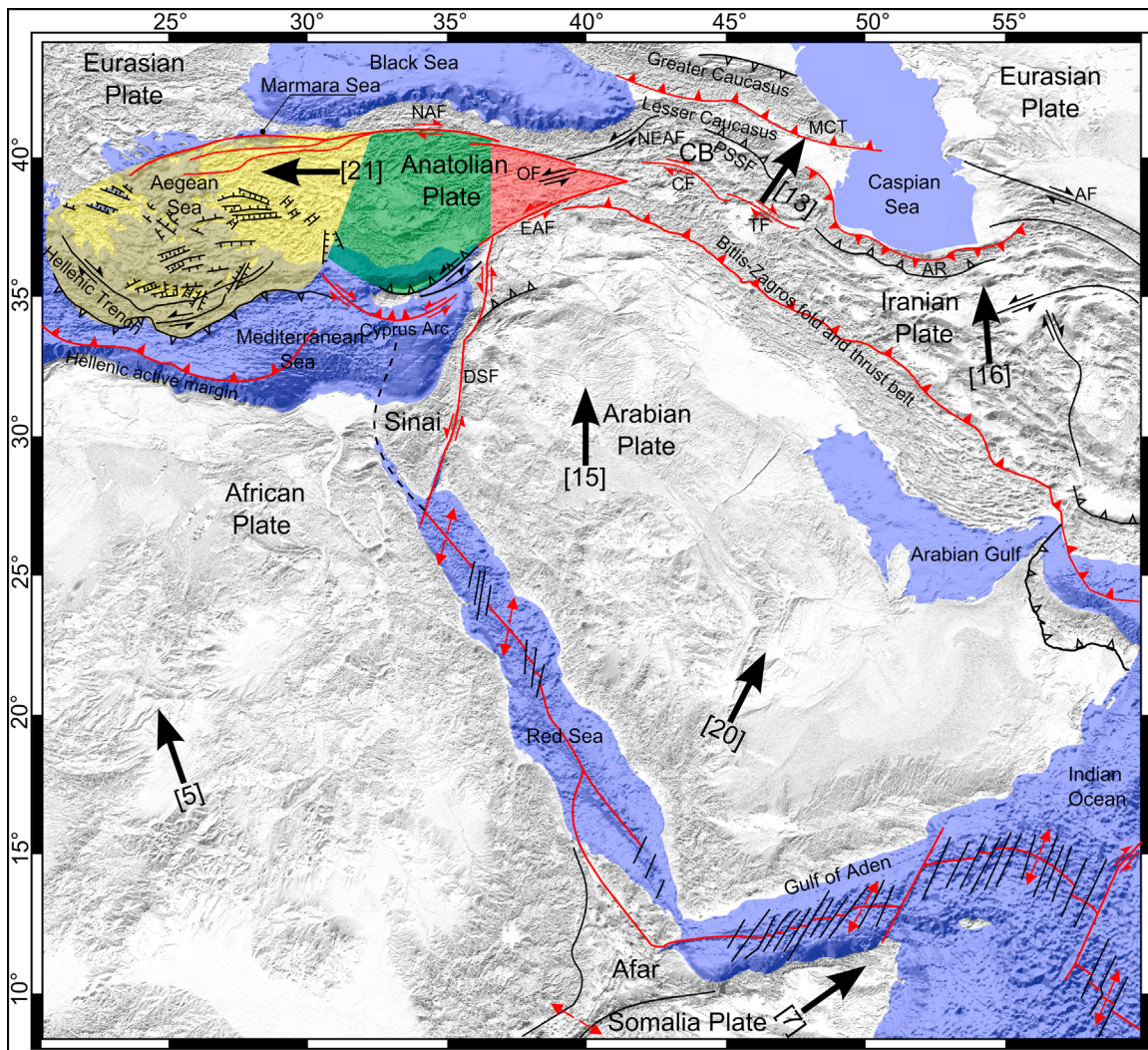


Figure 1. Map of the Anatolian plate region. A shaded relief map has been overlain with the location of faults. Dark arrows show the direction of plate motion based on GPS studies (relative to a fixed Eurasia), with the mm/yr shown in brackets [Reilinger *et al.*, 2006]. Red lines depict present plate boundary faults, and black lines are important faults. DSF, Dead Sea fault; NAF, North Anatolian Fault; EAF, East Anatolian fault; NEAF, northeast Anatolian fault; MCT, Main Caucasus thrust; AR, Alborz Range; CB, Caucasus Block; CF, Chalderan Fault; TF, Tabriz Fault; AF, Ashgabat Fault; PSSF, Pembak-Sevan-Sunik Fault; and OF, Ovacik fault. The three principal provinces of the Anatolian plate are shown with yellow, green, and red transparent overlays crudely reflecting the zonation of Şengör *et al.* [1985] into the western Anatolian extensional province, the central Anatolian Ova province, and the east Anatolian contractional province, respectively (see text for discussion).

about 85 km [Hubert-Ferrari *et al.*, 2009; Şengör *et al.*, 2005].¹ The age of the onset of faulting is determined by studying the age of sedimentary basins that formed due to the propagation and development of the NAF. It has been suggested that the NAF nucleated in the east around 13 Ma [Şengör *et al.*, 1985] and migrated westward reaching the Sea of Marmara around 5 Ma [Armijo *et al.*, 1999; Hubert-Ferrari *et al.*, 2002]. Others argue that the principal (northern) fault strand in the Sea of Marmara was not established until 200 ka [Şengör *et al.*, 2005]. There is still some uncertainty surrounding the age of strike-slip faulting

along the NAF [Uysal *et al.*, 2006]. The eastern end of the NAF has evolved in response to changes in the amount of deformation accommodated on various conjugate structures, namely the currently dominant East Anatolian Fault and previously dominant Ovacik Fault (Figure 1) [Hubert-Ferrari *et al.*, 2009; Westaway, 2003].

2.3. Fault Geometry and Segmentation

[10] The arcuate geometry of the NAF extends from the Karlova triple junction in the east into the Aegean Sea. Compared to other long strike-slip fault zones (e.g., the San Andreas and Alpine faults), the NAF has a relatively simple geometry, but there are complexities along its trace. Fault geometry is the major control on fault segmentation. Fault

¹Auxiliary materials are available in the HTML. doi:10.1029/2009JB006982.

Table 1. Summary of NAF Recurrence Interval Estimates^a

Location	Number of Events	Recurrence Interval (years)	Reference ^b
Kavakköy	4	~283±113	<i>Rockwell et al.</i> [2009]
Yenice-Gönen	4?	660±160	<i>Kürçer et al.</i> [2008]
Gölcük	3	210 and 280	<i>Klinger et al.</i> [2003]
Köseköy	4	~150	<i>Rockwell et al.</i> [2009]
Lake Efteni Düzce fault	5	400–500	<i>Sugai et al.</i> [2001]
Gerede	4	250–300	<i>Okumura et al.</i> [2002]
Ilgaz	5	280–620	<i>Sugai et al.</i> [1999]
Elmacik	7	97–912 (2σ)	<i>Fraser et al.</i> [2010]
Havza	3	600–900	<i>Yoshioka et al.</i> [2000]
Alayurt	4 or 5	250 to ≤ 800	<i>Hartleb et al.</i> [2003]
Destek	7	385°±166° (1σ)	<i>Fraser et al.</i> [2009]
Reşadiye	6	1–1375 (2σ) ^b	<i>Fraser</i> [2009]
Günalan	5	109–1385 (2σ)	<i>Fraser</i> [2009]
Yaylabeli	5	200 to <700	<i>Kozacı</i> [2008]
Çukurçimen	6 or 7	210 to <700	<i>Hartleb et al.</i> [2006]
East of Erzincan basin	8	200–250	<i>Okumura et al.</i> [1994a]

^aLocations are listed west to east. Results are directly quoted from relevant references.

^bA bimodal distribution was revealed with modes at 100–400 and 900–1200 years.

segments are sections of the fault separated by significant, potentially rupture-arresting, structural features. Segmentation affects how we correlate earthquake records along the fault. *Wesnowsky* [2006] studied historical continental strike-slip fault ruptures and found that fault steps of greater than 3–4 km arrest fault rupture, and smaller fault steps (i.e., < 3–4 km) arrest fault rupture about 40% of the time. Because of the 20th century earthquakes along most of the NAF, rupture segments can be identified and are defined as the section of the fault that ruptured during an individual earthquake. *Barka* [1996] described rupture segments of the earthquakes that occurred between 1939 and 1967 and further subdivided each rupture segment into fault segments based on geometry. Some segments may regularly rupture in unison with adjacent segments, and understanding the temporal continuity of these segments is fundamental in understanding the behavior of the NAF. The historical earthquake sequence is useful for determining fault segmentation, but because adjacent segments can rupture in unison during some seismic cycles these ruptures do not account for all of the segmentation. The geometry and segmentation of the NAF are not in the scope of this paper. We refer the reader to *Barka and Kadinsky-Cade* [1988], who provides a useful summary that identifies 69 fault segments, 26 of which are on the less complex central and eastern sections of the NAF (approximately east of Bolu) and the other 43 are along the furcated strands of the western section of the NAF. There are also many other papers that deal with segmentation of sections of the NAF [e.g., *Barka*, 1996; *Kondo et al.*, 2005; *Lettis et al.*, 2002].

2.4. Rate of Deformation

[11] Slip rate estimates have a considerable variability (Table S2) depending on how they are measured and the time period over which the rate is derived [*Kozacı et al.*, 2009]. GPS or geodesy based slip rates give a snap-shot of the strain accumulating across the NAF. Offset geomorphic, anthropogenic and geological piercing points give offsets over hundreds to millions of years, yielding an average rate of deformation over that period. Estimates of the rate of deformation from GPS-based studies vary slightly depending on model input data, the fault geometry

they use, and how much intraplate deformation they allow to occur. The GPS-based estimates of slip rate for the NAF are slightly higher than those based on geological and geomorphological observations. The higher rates from GPS are attributed to an unknown combination of post-seismic crustal relaxation (following the 20th century earthquake sequence [e.g., *Mantovani et al.*, 2007]) and account for deformation across the whole plate boundary, not just the principal fault strand. Variations in geological and geomorphological slip rates are attributed to along-strike variation, different durations of deformation relative to seismic cycles, inaccuracies in Quaternary dating methods, and perhaps temporal variation in slip rate. Aseismic creep has only been recognized on the ~70 km long Ismetpasa section of the NAF [*Barka*, 1992; *Cakir et al.*, 2005].

2.5. Recurrence Interval

[12] The recurrence interval is the time between subsequent earthquakes on a given fault segment; according to *Sieh* [1996, p. 3764] "... knowledge of the spatial and temporal complexity of earthquake recurrence is essential to an eventual understanding of the behavior of active faults and to reliable earthquake hazard evaluations and forecasts."

[13] Estimates of recurrence interval are presented as a range for a particular point of the fault where a study has been undertaken. This range takes into account the range in age of the intervals between earthquakes, and in the case of paleoseismologically determined earthquake ages, also the uncertainty associated with determining these ages. Table 1 catalogs the existing estimates of recurrence interval for a range of sites along the NAF. If the progressive failure of the 20th century earthquake sequence is typical of the fault, then recurrence intervals should be similar along the entire fault. If the recurrence intervals are not comparable, then the 20th century earthquake sequence may be atypical of the NAF. *Kozacı* [2008, p. 84] recognized that the interval between earthquakes "is not truly quasi-periodic" on the section of the fault that they studied, and in conjunction with other observations, they infer that the NAF "commonly, but not always, ruptures in clusters lasting on the order of a century." *Hartleb et al.* [2006, p. 823] too concluded that "the North Anatolian Fault does not always rupture in

sequences similar to the twentieth-century cluster," based on observations toward the eastern end of the NAF.

[14] Notably, the recurrence intervals listed in Table 1 have been calculated in a range of ways. As part of this study we re-calculate the recurrence intervals from selected investigations to produce probability density functions that describe the variation of the combined interval between earthquakes and the uncertainty associated with determining earthquake timing. This allows the most robust, consistent, and contemporary evaluation of the recurrence interval and provides an additional perspective on the long-term behavior of the NAF.

2.6. Displacement per Event

[15] Displacement per event is seldom known for earthquakes older than the 20th century on the NAF, and even in these cases measurement of offsets were in many cases made years to decades after the earthquake and thus include any post-co-seismic slip. Right-lateral offsets associated with recent earthquakes are summarized in Figure 2a. Displacements associated with older earthquakes are only documented at locations where detailed studies of geological or geomorphological features have been undertaken. In such studies the degree of certainty concerning the amount of offset caused by a particular paleoearthquake becomes less with time. At Ilgaz, near the western end of the 1943 rupture segment, *Sugai et al.* [1999] estimated the offset of the last three earthquakes (interpreted as historical earthquakes in A.D. 1943, 1668, and 1050) as 2.5–3.0 m, 5.0–6.0 m, and 5.0–6.0 m, respectively. A geomorphic study nearby revealed an offset of 46 ± 10 m formed over approximately 2 ka, which indicates that the most recent earthquake was probably uncharacteristically small [*Kozaci et al.*, 2007]. Nearer the middle of the 1943 rupture segment at Elmacik, *Fraser et al.* [2010] determined that average right-lateral offset caused by historical earthquakes in A.D. 1050 and 1668 was ~ 10 m based on subtraction of the 1.4 m to 2.6 m of offset measured near the investigation site following the 1943 earthquake [*Barka*, 1996]. This evidence suggests that at least the 1943 rupture of the 20th century earthquake sequence was uncharacteristically small and that the amount of offset, on that rupture segment, varies significantly between seismic cycles. These observations on the 1943 rupture segment suggest that the displacement per event may vary by nearly an order of magnitude. However, *Kondo et al.* [2004] describe characteristic slip events on the 1944 rupture with offsets of 4–5 m in 1944, 4.8 ± 1.5 m in A.D. 1668, 5.3 ± 2.3 m in 11th to 13th centuries A.D., and possibly 4.7 ± 0.9 m in A.D. 1035. Therefore, observations on the 1943 and 1944 rupture segments suggest that the behavior of the NAF varies along strike.

2.7. Historical Earthquake Record

[16] Figure 2b shows the extent of surface-rupturing earthquakes from the 20th century along the NAF. Table A1 summarizes published references to historical earthquakes that may be associated with surface rupture along the NAF [*Ambraseys*, 2002, 1970; *Ambraseys and Finkel*, 1987, 1991, 1995; *Ambraseys and Jackson*, 1998; *Ambraseys*, 2001; *Guidoboni et al.*, 1994; *Guidoboni and Comastri*, 2005; *Nur and Cline*, 2000; *Nur and Burgess*, 2008; *Stein et al.*, 1997; *Tibi et al.*, 2001]. Many of the reported earth-

quakes come from near Erzincan in the east and Istanbul in the west, while the records from the central portion of the NAF are sparser. This could be interpreted to reflect the distribution of earthquakes, spatial variation in record preservation, or a combination. The long and fascinating history of the NAF region is typified by regular movement of peoples, which can affect the creation and preservation of historic records.

3. Paleoseismic Earthquake Record

3.1. Procedure

[17] At least 55 paleoseismic trenching and coring studies have been conducted on the NAF (Figure 2b), and other studies are ongoing. In this section we describe the procedure that we use to compile and analyze the paleoseismic data. The procedure is summarized with a flow diagram (Figure 3) that also shows the figures, tables and auxiliary tables produced at each stage. The objective of compiling the paleoseismic data on the NAF is (1) to bring together all of the existing data into one accessible data set, (2) to identify gaps in the existing data set to focus further studies, and (3) to compile a data set using a standardized methodology to allow comparisons to be made between the results of paleoseismic investigations and between paleoseismic investigation data and the historical earthquake record.

3.1.1. Data Compilation

[18] The objectives require two data sets to be compiled from the existing published paleoseismic investigations along the NAF. One data set comprises all of the paleoseismic data from the NAF. These data are tabulated by investigation site showing the dated samples and event horizons in stratigraphic order (Table S3). These data come from the published papers on the NAF, but in some cases our interpretation differs from that of the original publication. Given the restrictions on the volume of analysis that can be presented in a single journal paper, we have only presented a single plausible interpretation of the published data. However, this is not to say that there are not other plausible interpretations. Documenting the consequences of different interpretations of each study is beyond the scope of this study. A subset of the paleoseismic investigations are selected for further analyses based on the number of paleoearthquakes, accuracy of temporal constraint, and location. Notes from the review process are presented in Appendix B and describe our interpretation of paleoseismic investigations, and which data are included in the subset for analysis. This review is summarized in Table 2 and the locations of investigations are shown in Figure 2 (using reference labels from Table 2).

3.1.2. Determining Paleoearthquake Timing

[19] OxCal input files were constructed for the studies selected for further analysis (a zip folder of files derived from the OxCal analysis undertaken in this study can be downloaded from an external ftp server at <ftp://omaftp.oma.be/dist/astro/Vanneste.K/2009JB006982R/>; in the subfolders, one for each study reanalyzed in this study, there are four files which can be opened using the program OxCal; the files with the extension .oxcal are the input files for the program OxCal, and files with the extensions .js, .log, and .txt are outputs from the program Oxcal). OxCal [*Bronk Ramsey*, 2007] is a radiocarbon age calibration software that we use to determine

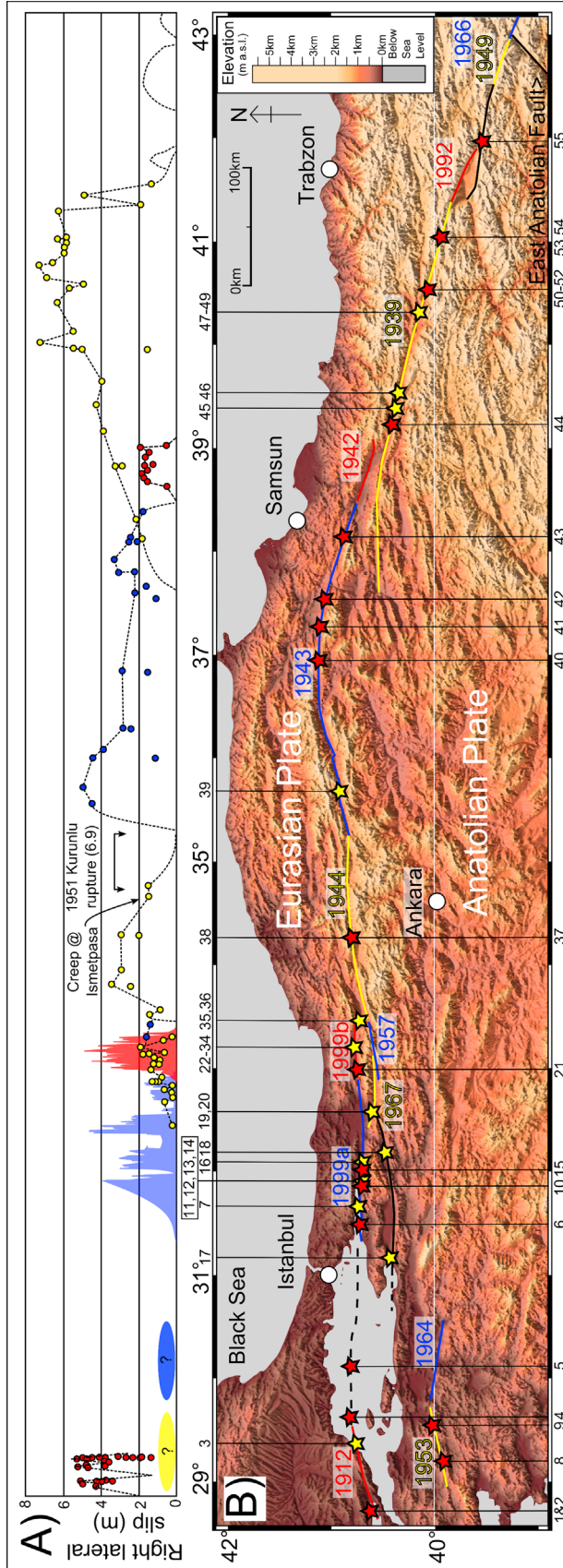


Figure 2. (a) Summary of right-lateral displacements caused by the major earthquakes in the 20th century on the NAF. Offset data for earthquakes in 1939, 1942, 1943, 1944, 1951 (location only), 1957 and 1967 are from *Barka* [1996]; 1992, 1966 and 1949 are from *Stein et al.* [1997]; offset data for the 1999 Izmit earthquake (1999a, blue filled) are from *Barka et al.* [2002]; Düzce earthquake (1999b, red filled) offset data are from *Akyüz et al.* [2002]; and the offset associated with the 1912 earthquake is from *Altunel et al.* [2004] although one measured offset extends to the west of the figure. No data have been located concerning the offsets associated with the 1953 and 1964 earthquakes at the western end of the NAF. The horizontal scale is east–west distance along the fault (i.e., no north–south component of distance is considered) with the same scale as Figure 2b. (b) Map of the NAF showing the location of paleoseismic investigations listed (yellow star, study number at top of map) and used in this study (red star, study number at the bottom of the map). Study numbers correspond to Table 2. Segments of the fault that have ruptured relatively recently are shown with colored lines (color corresponding to offset curves in Figure 2a) and are annotated with the year of rupture.

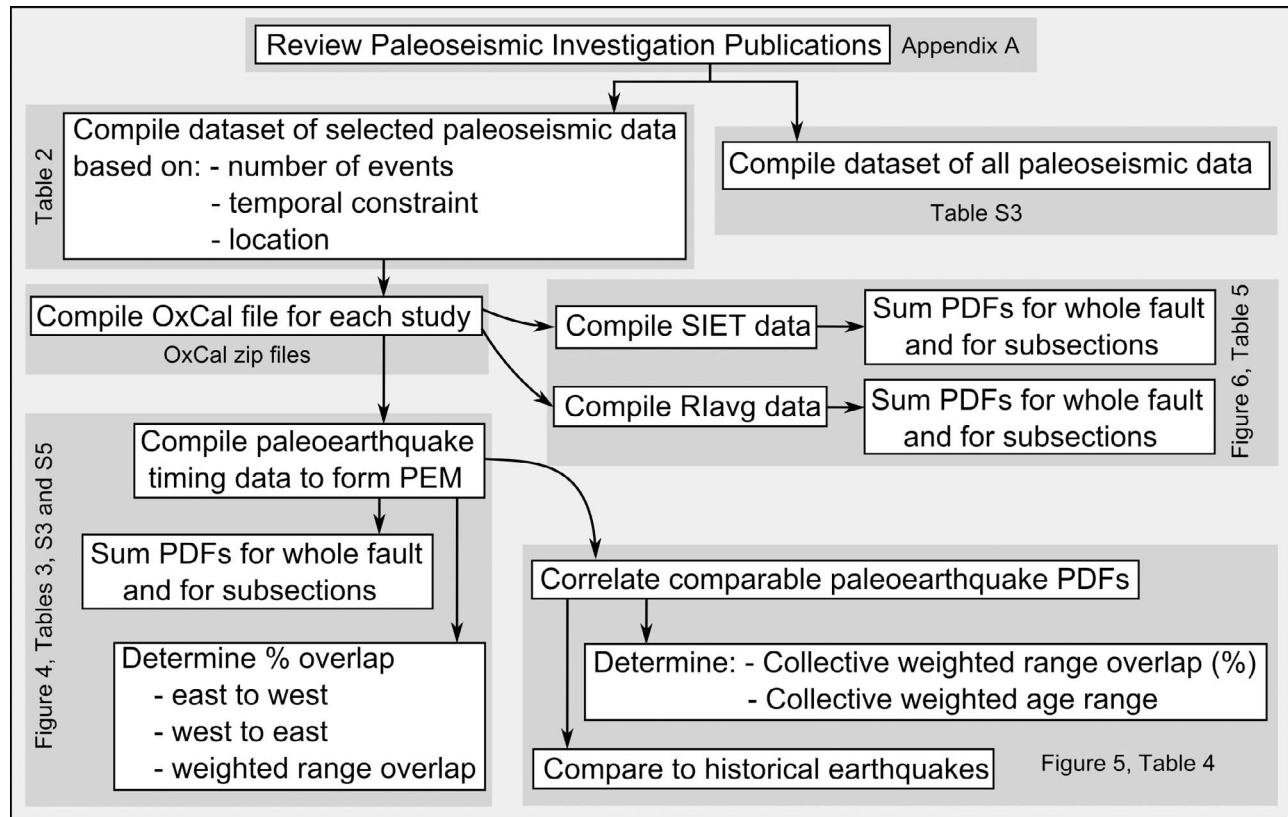


Figure 3. Flow diagram outlining the procedure used to analyze paleoseismic data, gray shading links results to figures, tables, and auxiliary material tables. SIET is summed interevent time, RIavg is average recurrence interval, PDF is probability density function, and PEM is paleoearthquake model.

probability density functions (PDFs) for the timing of paleoearthquakes (paleoearthquake PDFs). The input files use unrounded radiocarbon ages where possible. This is to determine the timing of earthquakes as accurately as possible, but in many cases conventional radiocarbon dates [Stuiver and Polach, 1977] had to be used. Calibration to calendar ages was based on the IntCal-04 calibration curve [Reimer et al., 2004], except for the studies from the Sea of Marmara, which use the Marine_04 calibration curve [Hughen et al., 2004]. We use a method similar to that of Lienkaemper and Bronk Ramsey [2009] to build the OxCal files. Each of the models uses stratigraphic ordering constraints; this utilizes the logic that samples from a given layer must be older than samples from the layer above [Biasi et al., 2002; Hilley and Young, 2008a]. In OxCal, this is achieved by entering the constraining dates, from oldest to youngest, in a “Sequence.” Where there are many samples in one layer, which may have been deposited relatively rapidly, or where the samples are from different locations in the trench making it difficult to establish their relative order, the sample ages are grouped into a “Phase,” in which stratigraphic order is not defined. In each sequence, we include a start and an end boundary. Where applicable, the likelihood for the end boundary is defined by the age of a 20th century earthquake. Not including boundaries would mean that all dates in the sequence are assumed to be entirely independent, apart from the applied constraint [Bronk Ramsey, 2007]. In such models, the posteriors can be unrealistically shifted away from each other [Steier and

Rom, 2000]. We note that Biasi et al. [2002] and Hilley and Young [2008a] did not use boundaries in their formulations, although Hilley and Young [2008a] observed a systematic aging of posterior layer PDFs with age in sequences ending with a known historical earthquake where the additional constraint of a minimum amount of time between layers (based on peat growth rates) was applied. Where an event horizon is identified in the stratigraphy, we use the “Date” command to generate a PDF that describes the paleoearthquake timing (paleoearthquake PDF). OxCal assumes a constant prior for such dates, which is then constrained by the PDFs of samples or phases above and below using Bayesian statistics. In essence, this is not entirely correct, since the event priors also influence the sample and phase posteriors, and hence also the other event posteriors, which should not be the case [Hilley and Young, 2008a]. In practice, this probably does not make much difference. Figure 4a graphically shows the paleoearthquake PDFs, which we refer to collectively as the paleoearthquake model. Investigations are labeled with a 3-character identifier (Table 2) and the paleoearthquake PDFs are labeled from young to old (see color coding in Figure 4), with the youngest PDF being 0 if it occurred after A.D. 1900, otherwise it is labeled 1. Paleoearthquake PDF 4 at Kavakköy A and 2 at Yenice-Gönen have been magnified so that they can be seen. The 2σ range of probability (i.e., incorporating 95.4% of the uncertainty) of paleoearthquake PDFs are summarized in Table 3. OxCal generates agreement indices that describe the

Table 2. Summary of Paleoseismic Investigations on the NAF

Ref ^a	Site name	Trench Location(s) UTM			Reference(s)	Distance ^b (km)	In Model?	Number of Events	Number of Trenches
		Zone	Easting	Northing					
1/KKA	Kavakköy A	35 T	488170	4495450	<i>Rockwell et al.</i> [2001]	200	Y	5	5
2/KKB	Kavakköy B	35 T	488170	4495450	<i>Rockwell et al.</i> [2009]	200	Y	4	21
3	Sea of Marmara-Ganos Basin	35 T	531230	4511080	<i>McHugh et al.</i> [2006]	243	N	3	core
4/MST	Sea of Marmara-Tekirdag Basin	35 T	550610	4516740	<i>McHugh et al.</i> [2006]	262	Y	2	core
5/MSC	Sea of Marmara-Central Basin	35 T	584330	4519270	<i>McHugh et al.</i> [2006]	296	Y	3	core
6/MSH	Sea of Marmara-Hersek Peninsula	35 T	708630	4510600	<i>McHugh et al.</i> [2006]	420	Y	3	core
7	Sea of Marmara-Gulf of İzmit	35 T	721260	4512080	<i>McHugh et al.</i> [2006]	433	N	3	core
8/YGO ^c	Yenice-Gönen Fault: Seyvan	35 S	526230	4420110	<i>Kürçer et al.</i> [2008]	238	Y	2	1
9/YGO ^c	Yenice-Gönen Fault: Muratlar	35 T	550150	4435510	<i>Kürçer et al.</i> [2008]	262	Y	3	1
10/GOL	Gölcük	35 T	741590	4510490	<i>Klinger et al.</i> [2003]	453	Y	3	2
11	Döniz Evler	35 T	742100	4510000	<i>Pavrides et al.</i> [2006]	454	N	4	1
12	Aşağı Yuvacık	35 T	749100	4512700	<i>Pavrides et al.</i> [2006]	461	N	2	1
13	Mahmutpaşaçiftliği	35 T	750400	4512600	<i>Tutkun and Pavrides</i> [2001] as cited by <i>Pavrides et al.</i> [2006]	462	N	0	1
14	Kullar-Yaylacık	35 T	751400	4512600	<i>Pavrides et al.</i> [2006]	463	N	0	1
15/KSK	Köseköy	36 T	248990	4512370	<i>Rockwell et al.</i> [2001, 2009]	467	Y	3	6
16	Acısu	37 T	254300	4511500	<i>Pavrides et al.</i> [2006]	468	N	0	1
17	İznik-Mekece fault: Çerkeşli	35 T	749330	4479980	<i>Honkura and Isikara</i> [1991]	461	N	1	1
18	İznik-Mekece fault: Geyve	36 T	270810	4485880	<i>Yoshioka and Kuşçu</i> [1994]	489	N	>1	1
19	Mudurnu Valley: Çakaloğlu	36 T	306165	4495410	<i>Ikeda et al.</i> [1991]	524	N	2	1
20	Mudurnu Valley B	36 T	308133	4494990	<i>Palyvos et al.</i> [2007]	526	N	3	1
21/DLE	Düzce fault: Lake Efteni	36 T	333720	4513980	<i>Sugai et al.</i> [2001]	552	Y	5	1
22	Düzce Fault A: Aksu	36 T	327480	4513790	<i>Pucci</i> [2006] and <i>Pantosti et al.</i> [2008]	545	N	3	1
23	Düzce Fault A: Cinarlı	36 T	340640	4514450	<i>Pucci</i> [2006] and <i>Pantosti et al.</i> [2008]	559	N	3	1
24	Düzce Fault A: Cakir Hacı Ibrahim	36 T	342290	4514450	<i>Pucci</i> [2006] and <i>Pantosti et al.</i> [2008]	560	N	3	1
25	Düzce Fault A: Mengencik 1	36 T	351980	4515220	<i>Pucci</i> [2006] and <i>Pantosti et al.</i> [2008]	570	N	3	1
26	Düzce Fault A: Mengencik 5	36 T	351980	4515220	<i>Pucci</i> [2006] and <i>Pantosti et al.</i> [2008]	570	N	2	1
27	Düzce Fault A: Mengencik 6	36T	352220	4515220	<i>Pucci</i> [2006] and <i>Pantosti et al.</i> [2008]	570	N	3	1
28	Düzce Fault A: KAY	36 T	357710	4515260	<i>Pucci</i> [2006] and <i>Pantosti et al.</i> [2008]	576	N	4	1
29	Düzce Fault B: Kaledibi	36 T	343640	4514780	<i>Komut</i> [2005]	562	N	0	1
30	Düzce Fault B: Bend	36 T	351040	4515270	<i>Komut</i> [2005]	569	N	0	2
31	Düzce Fault B: Tongelli	36 T	351620	4515210	<i>Komut</i> [2005]	570	N	0	2
32	Düzce Fault C: T1	36 T	359410	4515120	<i>Hitchcock et al.</i> [2003]	577	N	2	1
33	Düzce Fault C: T2	36 T	359910	4515100	<i>Hitchcock et al.</i> [2003]	578	N	3	1
34	Düzce Fault C: T3	36 T	360614	4515020	<i>Hitchcock et al.</i> [2003]	579	N	3	1
35	Bakacak Fault: sag pond	36 T	369210	4511710	<i>Hitchcock et al.</i> [2003]	587	N	3	1
36	Elmalik Fault: T2	36 T	369680	4509530	<i>Hitchcock et al.</i> [2003]	588	N	2	1
37/GDT	Gerede: Demir Tepe	36 T	443450	4519350	<i>Kondo et al.</i> [2004]	661	Y	4	1
38	Gerede: Arıdıclı	36 T	444420	4519330	<i>Okumura et al.</i> [2003]	662	N	6	1
39/IGZ	Ilgaz	36 T	543020	4536740	<i>Sugai et al.</i> , 1999]	761	N	5	3
40/ELM	Elmacık	36 T	659230	4552380	<i>Fraser et al.</i> [2010]	877	Y	7	1
41/HAV	Havza	36 T	721980	4544330	<i>Yoshioka et al.</i> [2000]	940	Y	3	1
42/AYA/AYB	Alayurt	36 T	740970	4538550	<i>Hartleb et al.</i> [2003]	959	Y	6	8
43/DTK	Destek	37 T	257400	4528190	<i>Fraser et al.</i> [2009]	982	Y	7	1
44/RSA	Reşadiye A	37 T	347170	4476200	<i>Fraser</i> [2009]	1072	Y	7	1
45	Umurca	37 T	349720	4475120	<i>Zabci et al.</i> [2008]	1075	N	3	1
46	Reşadiye B	37 T	378550	4464300	<i>Zabci et al.</i> [2008]	1104	N	3	2
47	Asagiyeniköy	37 T	458220	4433380	<i>Zabci et al.</i> [2008]	1184	N	2	2
48	Yukarıtepecik	37 T	462660	4432980	<i>Okumura et al.</i> [1994b]	1188	N	0	?
49	Asagi Tepecik	37 T	463900	4433220	<i>Zabci et al.</i> [2008]	1189	N	3	1
50	Günalan: T1	37 T	467390	4430960	<i>Fraser</i> [2009]	1192	N	1	1
51	Günalan: T2	37 T	467910	4430730	<i>Fraser</i> [2009]	1193	N	2	1
52/GUN	Günalan: T3	37 T	469160	4430180	<i>Fraser</i> [2009]	1194	Y	6	1

Table 2. (continued)

Ref ^a	Site name	Trench Location(s) UTM			Reference(s)	Distance ^b (km)	In Model?	Number of Events	Number of Trenches
		Zone	Easting	Northing					
53/YAY	Yaylabeli	37 S	494810	4423150	<i>Kozacı</i> [2008]	1220	Y	5	4
54/CUK	Çukurçimen	37 S	497960	4422480	<i>Hartleb et al.</i> [2006]	1223	Y	7	6
55/EEB	East Erzincan Basin	37 S	573520	4384350	<i>Okumura et al.</i> [1994a]	1299	Y	5	2

^aArbitrary reference number or abbreviation, corresponding to Figure 2.

^bWest to east distance along the fault from an arbitrary point in the Aegean Sea along a west to east line with no north to south component.

^cResults from these two trench sites are integrated for the paleoearthquake model.

model fit to the data (Table 4); values above 60 are considered to be acceptable. The results from the paleoseismic investigation at Ilgaz [*Sugai et al.*, 1999] are shown in Figure 4a and Table 3 because of the strategic position of this study on the NAF; but because the underlying dating data have not been published, unfortunately these data have not been modeled.

3.1.3. Comparing Paleearthquakes Between Investigations

[20] To analyze the relationships between the PDFs of different paleoseismic investigations, the paleoearthquake PDFs (Figure 4a) are summed along the whole NAF and along subsections (Figure 4b). The subsections are: the 1939 rupture segment (sites RSA, GUN, YAY, and CUK), the 1943 rupture segment (sites ELM, HAV, AYB, and DTK), and the western section of the NAF (sites KKB, YGO, MST, MSC, MSH, GOL, KSK, DLE, and GDT). The fault section east of the Erzincan basin was excluded because there is only one site (EEB). Notably, for all of the summed curves in Figure 4b we exclude several paleoearthquakes that have extremely long PDFs (noted in Table 3) due to unfavorable bounding dates. We exclude the record from Kavakköy A because the record from Kavakköy B is more recent and incorporates the data from Kavakköy A. We use the model Alayurt A rather than Alayurt B because this scenario for paleoearthquake 2 fits better with adjacent studies despite the preference of *Hartleb et al.* [2003] for model Alayurt B. To investigate the influence of the shape of the probability distribution between the 2σ uncertainty limits of the paleoearthquake PDFs, we also show summed curves determined by giving each paleoearthquake PDF a uniformly distributed probability between the 2σ uncertainty limits (Figure 4c). Hereafter, we assume that the error from other sources is negligible relative to the errors associated to radiocarbon dating.

[21] To determine the amount of overlap between paleoearthquake PDFs from different investigation sites, we use two measures of overlap described by *Hilley and Young* [2008b] to compare paleoearthquake PDFs on the San Andreas Fault. The first measure is a modification of the “mean event overlap,” where we calculate the cumulative probability of the 2σ range of each PDF that falls in the 2σ range of the other. This value depends on the order in which PDFs are compared. We calculated the overlap for each possible pair of correlating paleoearthquakes (except for paleoearthquakes from the same investigation site), once with the western site first, and once with the eastern site first. The mean event overlap is then the mean of these two values. The results of this analysis are tabulated in Table S4, where every paleoearthquake PDF is listed on the horizontal and vertical axis, and the percentage overlap is shown at the

intersection for the west to east directed analysis on the upper right half of Table S4 and east to west on the left lower half of Table S4. The second measure of overlap is the “weighted range overlap,” which was first introduced by *Biasi et al.* [2002]. It is the cumulative of the minimum probability of the two compared paleoearthquake PDFs at each time. This value is independent of comparison order and is tabulated in Table S5.

3.1.4. Comparing Paleearthquakes to Historical Earthquakes

[22] To compare the paleoearthquake PDFs to historical earthquakes we have mostly used a qualitative analysis. Historical earthquakes correlated to paleoearthquakes according to the original publications are listed in Table 3. Our correlation of the paleoearthquake PDFs in the paleoearthquake model is shown in Figure 5, and plausible correlating earthquakes are listed in Table 5. To investigate how well the correlated paleoearthquake PDFs correspond to each other, we extend the “weighted range overlap” described by *Hilley and Young* [2008b] to take into account more than two PDFs. We call the percentage of the multiple PDFs that overlap the collective weighted range overlap, and the period over which they overlap the collective weighted age range. In essence, the collective weighted age range is similar to the PDF obtained by multiplying supposedly correlating paleoearthquake PDFs. Therefore, if one of the paleoearthquake PDFs has a value of 0 for a particular year, then the collective weighted range for that year is 0. These data are listed in Table 5.

3.1.5. Determining and Comparing Recurrence Intervals

[23] At the end of each OxCal input file, query commands can be inserted to calculate dependent parameters of the model. Similar to *Lienkaemper and Bronk Ramsey* [2009], we thus determine the summed interevent time (SIET) and the average recurrence interval (RIavg), which are calculated in different ways, but both described with PDFs. The SIET is determined for each site by summing PDFs of the interevent time. This is described by *Lienkaemper and Bronk Ramsey* [2009, p. 433] as the method to determine the “variation about the mean recurrence interval,” and summarizes the variability of the interevent time along with the error associated with dating the age of the paleoearthquakes. The RIavg is determined by dividing the time between the oldest and youngest paleoearthquakes in the trench by the number of intervening interevent times (i.e., number of earthquakes minus one). *Lienkaemper and Bronk Ramsey* [2009, p. 433] call this “mean recurrence interval,” and it provides a very simplified recurrence interval that does not take into account the variability of interevent times

Table 3. Summary of Paleoearthquake Timing Based on Paleoseismic Data Compared to Historical Earthquakes Attributed to Events in Original Publications^a

Paleoearthquake	Paleoearthquake Timing (years A.D./B.C.) 2σ	Historical Earthquake ^b
KKA0 ^c	A.D. 1912	Superseded by
KKA1 ^c	A.D. 1478–1911	Kavakköy B
KKA2 ^c	A.D. 895–990	
KKA3 ^c	A.D. 788–943	
KKA4 ^c	2363 B.C. to A.D. 375	
KKB0	A.D. 1912	A.D. 1912 (30)
KKB1	A.D. 1658–1800	A.D. 1766 (43)
KKB2	A.D. 1029–1411	A.D. 1344 (79)
KKB3	A.D. 829–1112	A.D. 1063 (95)
YGO0	A.D. 1953	A.D. 1953 (15)
YGO1	A.D. 1225–1376	nc
YGO2 ^c	2923 B.C. to A.D. 650	nc - wide distribution
MST0	A.D. 1912	A.D. 1912 (30)
MST1	A.D. 1053–1286	A.D. 1063 (95)
MSC0	A.D. 1912	A.D. 1912 (30)
MSC1	A.D. 829–1418	A.D. 1343 (80 or 81)
MSC2	A.D. 644–904	A.D. 740 (109)
MSH1	A.D. 1830–1951	A.D. 1894 (33)
MSH2	A.D. 1705–1905	A.D. 1766 (43 or 44)
MSH3	A.D. 1524–1713	<i>A.D. 1509</i> (71)
GOL0	A.D. 1999	A.D. 1999 (2)
GOL1	A.D. 1539–1825	A.D. 1719 (49)
GOL2	A.D. 1357–1548	A.D. 1509 (71)
KSK0	A.D. 1999	A.D. 1999 (2)
KSK1	A.D. 1826–2000	A.D. 1754, 1878 or 1894 (46, 34.5, 33)
KSK2	A.D. 1711–1930	A.D. 1719 (49)
DLE0	A.D. 1999	A.D. 1999 (1)
DLE1	A.D. 1551–1929	nc
DLE2	A.D. 839–1232	nc
DLE3	A.D. 54–353	nc
DLE4	147 B.C. to A.D. 120	nc
GDT0	A.D. 1944	A.D. 1944 (19)
GDT1	A.D. 1675–1904	A.D. 1668 (52–54)
GDT2	A.D. 1116–1509	nc
GDT3	A.D. 790–987	<i>A.D. 1035</i> (99)
IGZ0 ^{c,d}	A.D. 1943	A.D. 1943 (20)
IGZ1 ^{c,d}	A.D. 1495–1850	A.D. 1668 (52–54)
IGZ2 ^{c,d}	A.D. 890–1190	A.D. 1050 (96)
IGZ3 ^{c,d}	A.D. 640–810	nc
IGZ4 ^{c,d}	0 to A.D.15	nc
ELM1	A.D. 550–651	<i>A.D. 529</i> (113)
ELM2	23 B.C. to A.D. 103	nc
ELM3	610–186 B.C.	nc
ELM4	971–813 B.C.	nc
ELM5	1228–969 B.C.	~1200 B.C. (143)
ELM6	2051–1777 B.C.	nc
ELM7	2556–2235 B.C.	nc
HAV0	A.D. 1943	A.D. 1943 (20)
HAV1	A.D. 1159–1374	not recognized
HAV2	A.D. 365–740	nc
HAV3 ^c	2330–1557 B.C.	nc, wide distribution
AYA0	A.D. 1943	A.D. 1943 (20)
AYA1	A.D. 1404–1805	A.D. 1668 (52–54)
AYA2	A.D. 1194–1381	nc
AYA3	A.D. 479–957	<i>A.D. 236</i> (129)
AYA4 ^c	1345 B.C. to A.D. 45	nc, wide distribution
AYB0 ^c	A.D. 1943	Alayurt scenario A preferred
AYB1 ^c	A.D. 1399–1806	
AYB2 ^c	A.D. 867–1112	
AYB3 ^c	A.D. 476–941	
AYB4 ^c	1344 B.C. to A.D. 47	
DTK0	A.D. 1943	A.D. 1943 (20)
DTK1	A.D. 1438–1787	A.D. 1668 or 1598 (52–54, 61)
DTK2	A.D. 1034–1325	nc
DTK3	A.D. 549–721	nc

Table 3. (continued)

Paleoearthquake	Paleoearthquake Timing (years A.D./B.C.) 2σ	Historical Earthquake ^b
DTK4	A.D. 17–585	A.D. 236, 499 (129, 114)
DTK5	351 B.C. to A.D. 28	nc
DTK6	705–392 B.C.	nc
DTK7	913–595 B.C.	nc
RSA0	A.D. 1939	A.D. 1939 (24)
RSA1	A.D. 1570–1939	A.D. 1668 (52–54)
RSA2	A.D. 261–642	A.D. 499 (114)
RSA3	257 B. C to A.D. 260	nc
RSA4	908–705 B.C.	nc
RSA5	2019–1804 B.C.	nc
RSA6	2280–2067 B.C.	nc
GUN0	A.D. 1939	A.D. 1939 (24)
GUN1	A.D. 1409–1803	A.D. 1668 (52–54)
GUN2	A.D. 1259–1391	<i>A.D. 1254</i> (85)
GUN3	A.D. 241–644	A.D. 499 (114)
GUN4	881–673 B.C.	nc
GUN5	1406–1291 B.C.	~1200 B.C.? (143)
YAY0	A.D. 1939	A.D. 1939 (24)
YAY1	A.D. 1132–1938	A.D. 1254 (85)
YAY2	A.D. 907–1077	A.D. 1045 (97)
YAY3	A.D. 756–876	nc
YAY4	A.D. 389–543	A.D. 499 (114)
CUK0	A.D.1939	A.D. 1939 (24)
CUK1	A.D. 1027–1428	A.D. 1254 (85)
CUK2	A.D. 929–1030	<i>A.D. 1045</i> (97)
CUK3	A.D. 365–523	A.D. 499 (114)
CUK4	303–57 B.C.	nc
CUK5	909–537 B.C.	nc
CUK6 ^c	2381–1504 B.C.	nc - wide distribution
EEB1	A.D. 1673–1950	A.D. 1784 (41)
EEB2	A.D. 1461–1639	nc
EEB3	A.D. 1323–1524	nc
EEB4	A.D. 1066–1275	nc
EEB5	A.D. 684–935	nc

^aPaleoearthquakes are labeled from the top downward, 0 is used for earthquakes of the most recent seismic cycle (i.e., post A.D. 1900). Paleoearthquake names correspond to site abbreviations in Table 1 where references can be found; nc, no correlation to historical earthquakes by the original authors.

^bThe year of a historical earthquake the original authors correlated to the paleoearthquake. The number in parentheses refers to the reference number column in Table A1. Italicized dates fall outside our modeled 2σ range for the paleoearthquake (this does not mean that it does not correlate).

^cNot used to determine RIavg, SIET, or summed curves.

^dThe results from Ilgaz are not modeled; that is, the results from the parent paper are directly quoted. Therefore, the uncertainty associated with the age ranges for earthquakes is not known.

determined in a study and only accounts for the dating uncertainty associated with the youngest and oldest events. Some paleoearthquake PDFs were too long (i.e., the timing of the paleoearthquake is poorly constrained) to include in determining the SIET and RIavg so they were excluded (as noted in Table 3). PDFs of the SIET and RIavg from each investigation site are summarized in Figure 6b and Table 5. To analyze spatial variation of the PDFs of SIET and RIavg, we summed the PDFs along the whole fault and along subsections of the fault (Figures 6c and 6d), similar to the way we summed the paleoearthquake PDFs. Because the PDFs of SIET and RIavg are based on different numbers of paleoearthquakes at each site, a weighting of how many interevent times were used to form the individual PDFs is applied to sum the SIET and RIavg (e.g., Elmacik has a

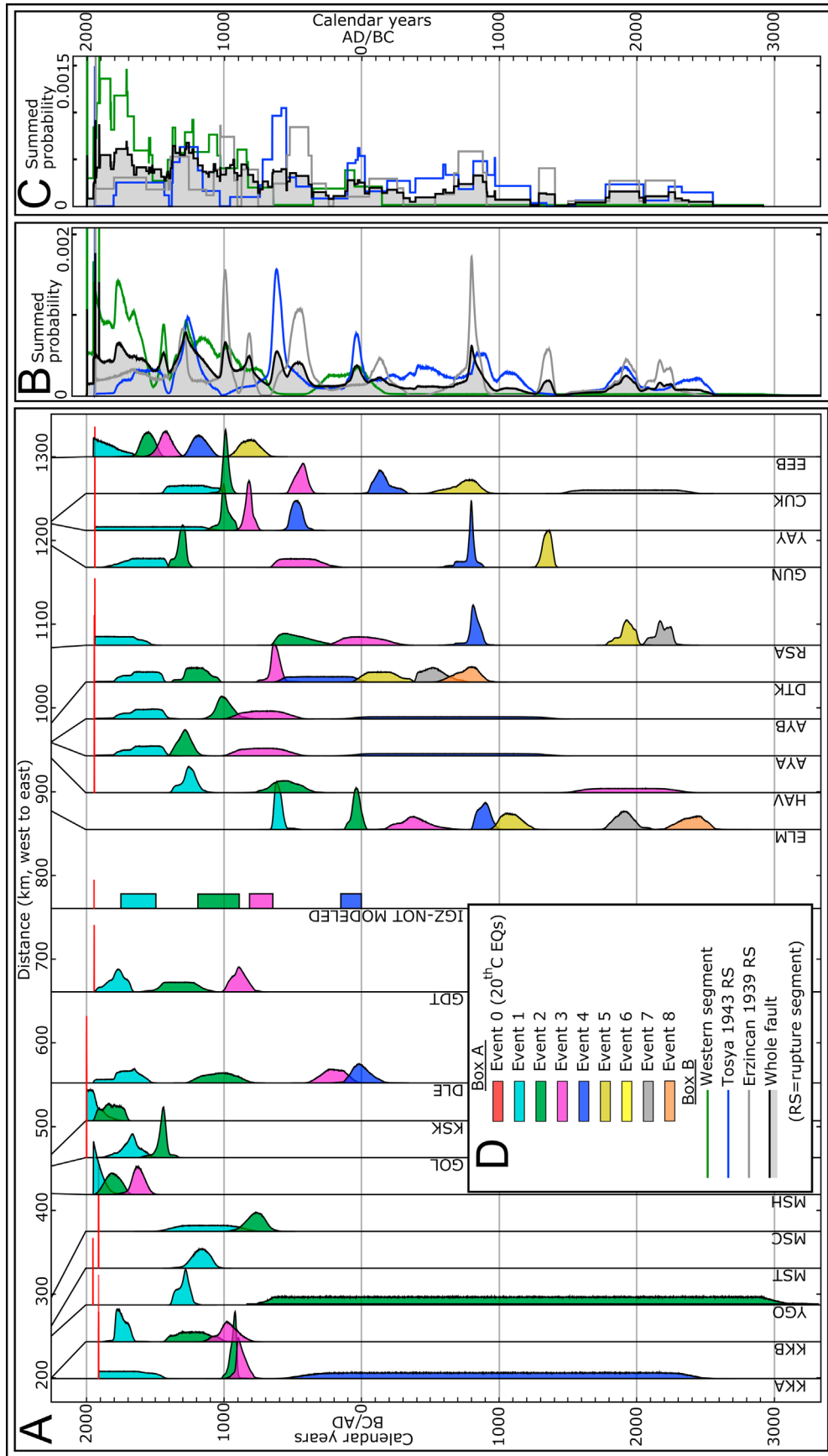


Figure 4. (a) Graph of annual paleoearthquake probability over time (vertical axis) and west-to-east distance along the fault (horizontal axis) based on re-interpreted paleoearthquake chronologies from selected preexisting paleoseismic studies along the fault. Each paleoearthquake PDF is uniquely identified by its number (color coded) and site abbreviation (at the base of the figure, see Table 2 for references). The 2σ ranges of the paleoearthquake PDFs are listed in Table 3. (b) Summed probability of paleoearthquake PDFs shown in Figure 4a. The lines each correspond to a summation of a selected subset of the data in Figure 4a (described in text). Some of the probabilities over the last 100 years extend beyond the area of this plot but do not exceed a value of 0.005. (c) Summed probability of the event timing based on a uniform probability distribution between the 2σ range of each event PDF for the same selected subsets of data as shown in Figure 4b (see text for description). Some of the probabilities over the last 100 years extend beyond this plot but do not exceed a value of 0.003. (d) Legend.

Table 4. Correlation of Paleoearthquakes to Each Other and to Historical Earthquakes

Ref	Paleoearthquake(s)	CWRO ^a (%)	CWR ^a	Historical Earthquake(s) ^b
1	DLE0	null	null	A.D. 1999 (1)
2	GOL0, KSK0	null	null	A.D. 1999 (2)
3	YGO0	null	null	A.D. 1953 (15)
4	GDT0	null	null	A.D. 1944 (19)
5	HAV0, AYA0, DTK0	null	null	A.D. 1943 (20)
6	RSA0, GUN0, YAY0, CUK0	null	null	A.D. 1939 (24)
7	KKB0, MST0, MSC0	null	null	A.D. 1912 (30)
8	KSK1, MSH1	50.8	A.D. 1714–1951	A.D. 1894, 1878 (33, 34.5)
9	EEB1	null	null	A.D. 1784 (41)
10	KKB1	null	null	A.D. 1766 (43)
11	MSH2, GOL1, KSK2, DLE1	27.8	A.D.1673– 1934	A.D. 1719, 1766 (49,44)
12	GDT1 ^c , AYA1, DTK1, RSA1, GUN1	22.0	A.D.1540–1918	A.D. 1668 (52–54)
12a	GDT1 ^c , AYA1, DTK1	24.00	A.D.1540–1943	A.D. 1579, 1590, 1598, 1668, 1776 (65, 63, 61, 54–52, 42)
12b	RSA1 ^d , GUN1	50.5	A.D. 1456–1918	A.D. 1543, 1684 (69, 50)
13	MSH3	null	null	A.D. 1556, 1593, 1625, 1648, 1672 (68, 62, 59, 58, 51)
14	GOL2	null	null	A.D. 1419, 1509 (76, 71)
15	EEB2	null	null	A.D. 1535, 1543, 1575, 1579, 1583, 1601 (70, 69, 66, 65, 64, 60)
16	KKB2, MSC1 ^c , MST1	46.0	A.D. 939–1443	A.D. 1063, 1090, 1162, 1231, 1237, 1265, 1296 1343, 1344, 1354 (95, 93, 91, 88, 86, 84, 78–82)
17	YGO1	null	null	A.D. 1265 (84)
18	EEB3	null	null	A.D. 1374, 1457, 1481 (77, 75, 74)
19	GUN2	null	null	A.D. 1287 (83)
20	YAY1, CUK1	41.5	A.D. 983–1616	A.D. 1254 (85)
21	GDT2, HAV1, AYA2, DTK2	37.9	A.D. 1062–1401	A.D. 1035, 1050 (99, 96)
22	EEB4	null	null	A.D. 1166, 1206, 1237 (90, 89, 87)
23	YAY2, CUK2	72	A.D. 889–1151	A.D. 1011, 1045 (97, 102)
24	GDT3	null	null	A.D. 967 (105)
25	KKB3, DLE2, MSC1	47.7	A.D. 717– 1240	A.D. 860, 869, 989, 1010, 1026, 1032 (107, 106, 104, 103, 101, 100)
26	MSC2	null	null	A.D. 740 (109)
27	YAY3, EEB4	0	null	nc
28	ELM1, HAV2, AYA3, DTK3 ^d	24.3	A.D. 434–752	A.D. 529 (113)
29	RSA2, GUN3, YAY4, CUK3	38.7	A.D. 261–596	A.D. 499 (114)
30	DTK4	null	null	A.D. 236 (129)
31	DLE3	null	null	A.D. 29, 68, 69, 121 (139, 137, 136, 135)
32	DLE4	null	null	A.D. 29, 68, 69 (139, 137, 136)
33	ELM2, AYA4 ^c , DTK5	5.5	103 B.C.– A.D. 164	Nc
34	CUK4, RSA3	39.6	357 B.C.–A.D. 58	Nc
nc	YGO3	null	null	Nc
35	ELM3, AYA4 ^c , DTK6	19.6	746–212 B.C	Nc
36	ELM4, AYA4 ^c , DTK7	10.1	1062–770 B.C.	Nc
37	RSA4, GUN4, CUK5	39.6	916–555 B.C.	Nc
38	ELM5 ^d , AYA4 ^c	21.9	1359–904 B.C.	~1200 B.C. (143)
39	GUN6	null	null	Nc
40	ELM6, HAV3 ^c	40.6	2193–1678 B.C.	Nc
41	RSA5, CUK6 ^c	29.2	2135–1705 B.C.	Nc
42	RSA6, CUK6 ^c	28.7	2454–1978 B.C	Nc
43	ELM7, HAV3 ^c	12.9	2522–2049 B.C.	Nc

^aCWRO, collective weighted range overlap; CWR, collective weighted age range.

^bThe reference number (in parentheses) corresponds to reference numbers used in Table A1; nc, no correlative event.

^cDenotes that correlations to multiple groups of paleoearthquakes have been made.

^dHistorical earthquake does not fall within 2σ range of paleoearthquake timing, but a correlation is still made.

weight of 6 and Havza a weight of 2). Furthermore, paleoseismic records Kavakköy A and Alayurt B are excluded from the summations in favor of Kavakköy B and Alayurt A, respectively.

3.2. Observations

[24] In this section we describe what the various analyses of the paleoearthquakes have revealed.

3.2.1. Comparison of Paleoearthquake Records

[25] The paleoearthquake timing (Figure 4a and Table 3) was summed along the whole NAF (Figure 4b) to reveal a

generally decreasing overall summed event probability over time due to decreasing data. There are several peaks in the data that are attributed to periods of higher activity along the studied sections of the NAF. Patterns become less clear over approximately the last 500 years, which we attribute to troughs in the radiocarbon calibration curve that cause broader sample age PDFs over this period, more results from along the whole NAF for this time period, and overlapping paleoearthquake PDFs at individual sites (e.g., MSH and KSK). By summing paleoearthquake probability along the three previously defined subsections of the NAF we observe

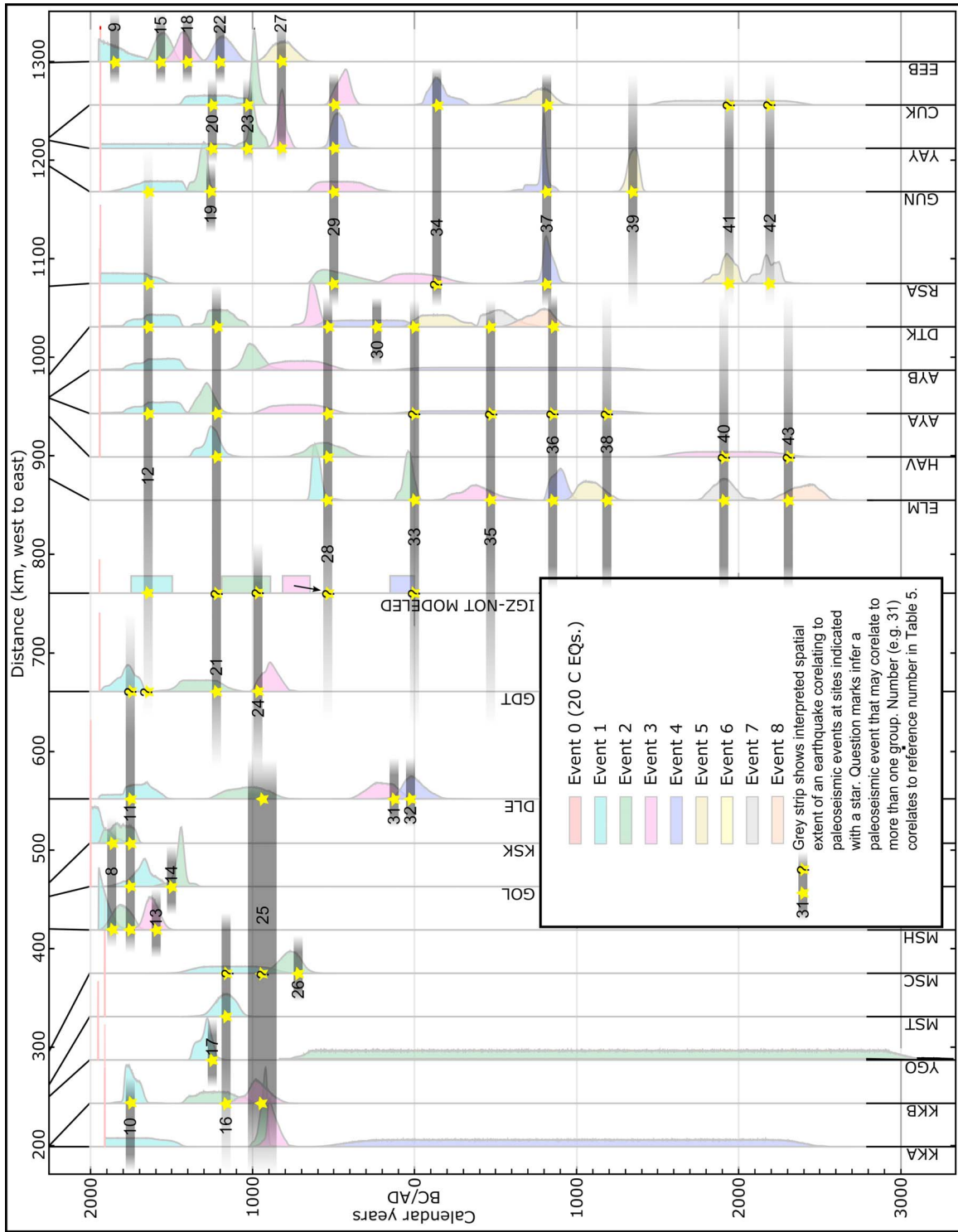


Figure 5. Graph showing the correlation of paleoearthquake PDFs (as presented in Figure 4) determined in this study with historical earthquakes (Table A1). The horizontal lines correspond to earthquakes listed in Table 4. Earthquake records come from published paleoseismic investigations and are labeled with abbreviations at the bottom that correspond to Table 2, which shows the investigation site full names, references, etc. Notice that correlations are not made with the records for Kavakköy A (KKA) or Alayurt B (AYB) (see text for discussion).

Table 5. Summary of Recurrence Interval Data Determined for Selected Investigations on the NAF Using OxCal^a

Site Reference	Number of Events	OxCal Indices		Average Recurrence Interval 2σ (years)	Summed Interevent Time 2σ (years)
		A_{model}	A_{overall}		
KKA	5 ^b	44.2	44.7	323–375	0–977
KKB	4	99.7	100.1	267–361	61–675
YGO	2 ^b	98.8	99	576–727	576–727
MST	2	70.8	71.6	625–859	625–859
MSC	3	105.9	99.6	504–633	77–1050
MSH	3	108.8	104.9	81–197	12–279
GOL	3	105.3	105.4	226–321	109–441
KSK	3	75.9	77.3	34–143	0–213
DLE	5	94.8	95.9	469–536	46–1010
GDT	4	98.4	98.7	478–576	54–652
ELM	7	78.2	81.5	470–529	98–913
HAV	4 ^b	93.6	94.4	601–789	520–890
AYA	5 ^b	104.8	104.8	329–488	110–768
AYB	5 ^b	104.5	104.6	334–489	57–770
DTK	8	107.6	107.5	362–407	60–689
RSA	7	60.2	68.8	667–702	0–1377
GUN	6	91.3	93.3	646–688	110–1386
YAY	5	24.5	27.4	349–387	51–859
CUK	7 ^b	114.5	115.5	495–570	92–857
EEB	5	158.2	156.2	202–306	43–491

^aNumber of iterations was manually increased to smooth resulting outputs (i.e., OxCal command: “KIterations = 100”).

^bThe last (oldest) paleoearthquake is poorly constrained and therefore is not used to determine average recurrence interval and summed interevent time.

that (1) the 1939 and 1943 rupture segments have much longer paleoearthquake records, (2) the pattern of seismicity on those rupture segments is relatively well constrained, and (3) the paleoearthquakes on those segments are closely spaced in time but clearly not always contemporaneous (e.g., around A.D. 500). Inherent in making these observations we assume that these earthquake records are complete (i.e., not missing events). This may not be the case, and new data may therefore affect our interpretation. On the 1939 rupture segment there are several paleoearthquakes between A.D. 500 and 1500 that only appear at the eastern end of the segment, suggesting that this segment does not always rupture in unison. On the 1943 segment it appears that the paleoearthquakes correlate well between studies, with the exception of the Havza site, which seems to miss a late second millennium A.D. paleoearthquake, and paleoearthquakes in the first 1500 years B.C., which was also observed by *Fraser et al.* [2010].

[26] Paleoearthquake PDFs describe the probability of event horizon age using only the uncertainty associated with radiocarbon ages (described by PDFs). Probability variations within a paleoearthquake PDF are determined by Bayesian constraints on the bounding dates, but also by variations in the shape of the calibration curve used to calibrate these bounding dates. The latter variations may not hold much meaning in terms of event probability, particularly considering that there are other possible sources of error which are not taken into account. Other possible sources of error may reflect misinterpretation of the strata or the unknown history of radiocarbon-dated samples (i.e., probable pre-deposition aging of samples, or possible younger samples deposited in the subsurface by bioturbation, desiccation or tectonic cracking). Therefore, the per-

turbations in paleoearthquake probability may affect the ability to correlate their PDFs. To investigate the effect of variation in probability, we replaced the paleoearthquake PDFs with uniform probability distributions between their respective 2σ uncertainty ranges, and summed them to create Figure 4c. Because the same patterns are revealed in Figures 4b and 4c, we suggest that the variation in probability between the 2σ uncertainty ranges of the paleoearthquake PDFs is relatively insignificant.

[27] The percentage overlap east–west and west–east is listed in Table S4, and the weighted range overlap is summarized in Table S5. Essentially these are quantitative comparisons of what can be ascertained visually (qualitatively) from Figure 4a.

3.2.2. Comparison of Paleoearthquakes to Historical Earthquakes

[28] Correlations between paleoearthquake PDFs that may reflect the same earthquake are shown graphically in Figure 5. Labels in Figure 5 are linked to Table 4, which lists the correlated paleoearthquake PDFs and the year of possible correlative historical earthquakes. Historical earthquakes attributed to particular paleoearthquakes in the parent publications of the paleoseismic data (see Table 2 for references) are listed in Table 3. Seven of the historical earthquakes to paleoearthquake correlations made in the original publications fall outside the 2σ range of the paleoearthquake PDFs (determined in this study). This does not necessarily mean that the correlation is inappropriate (e.g., radiocarbon samples, in some cases, may not reflect the age of the strata in which they are found due to reworking or contamination of the samples), although there are almost certainly significant earthquakes for which historical records do not exist. Because this is just a matter of matching known historical earthquakes, which may have occurred in the vicinity of the investigation site, to the paleoearthquake PDFs, it is difficult to do more with these data.

[29] Because earthquakes can occur closely spaced in time (e.g., 20th century sequence on the NAF) and can rupture variable lengths during each seismic cycle, it is presently impossible to know if correlated paleoearthquake PDFs from multiple investigation sites reflect individual rupture segments or segments that ruptured closely spaced in time. For this reason it is difficult to know if it is appropriate to use the timing constraints from multiple investigation sites to further constrain the timing of paleoearthquakes. To investigate this further, we determined the collective weighted range overlap and the collective weighted age range, which are listed in Table 4. Most of the historical earthquakes that we have correlated to paleoearthquakes fall inside the collective weighted age range regardless of the value of the collective weighted range overlap (%). This is an interesting observation, because it suggests that, with caution, the results from multiple paleoseismic investigations sites can be used to further constrain the timing of paleoearthquakes. However, particularly on faults where fault segmentation has not been clearly established, the distance between investigation sites used in unison must be clearly justified.

[30] The earthquakes of A.D. 1668 (Table A1), thought to be the largest known earthquake(s) on the NAF [*Ambraseys and Finkel*, 1995], are almost certainly attributable to a series of large ruptures along the NAF. It is not clear exactly

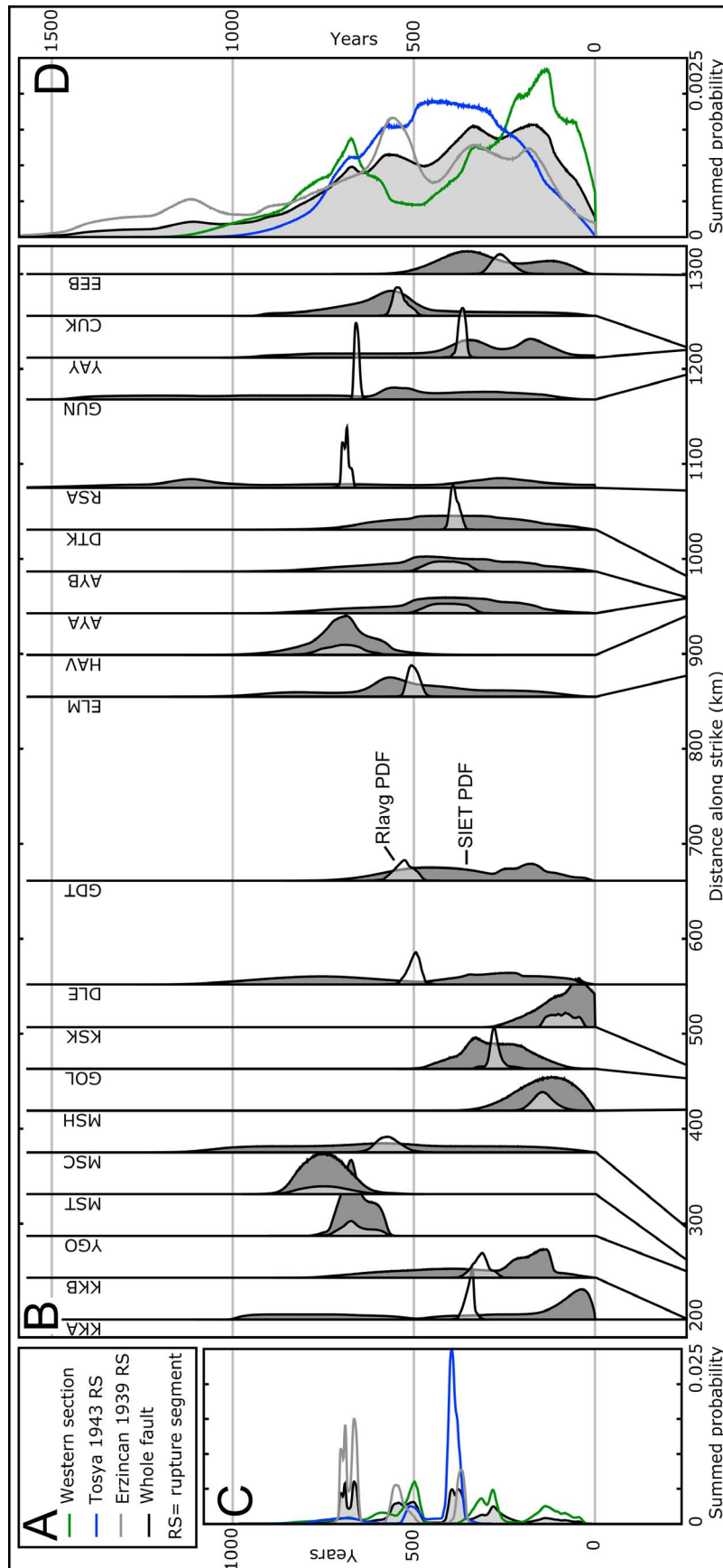


Figure 6. (a) Legend for Figures 6c and 6d. (b) PDFs of summed interevent time (SIET) (filled with dark gray) overlain with PDFs of average recurrence intervals (Rlavg) (no fill or lighter gray where overlapping with SIET) for selected paleoseismic investigations along the NAF (see text for discussion). (c) Summed probability of Rlavg for the whole NAF (light gray fill) and selected subsections of the fault. (d) Summed probability of the SIET for the whole NAF (light gray fill) and subsections of the fault.

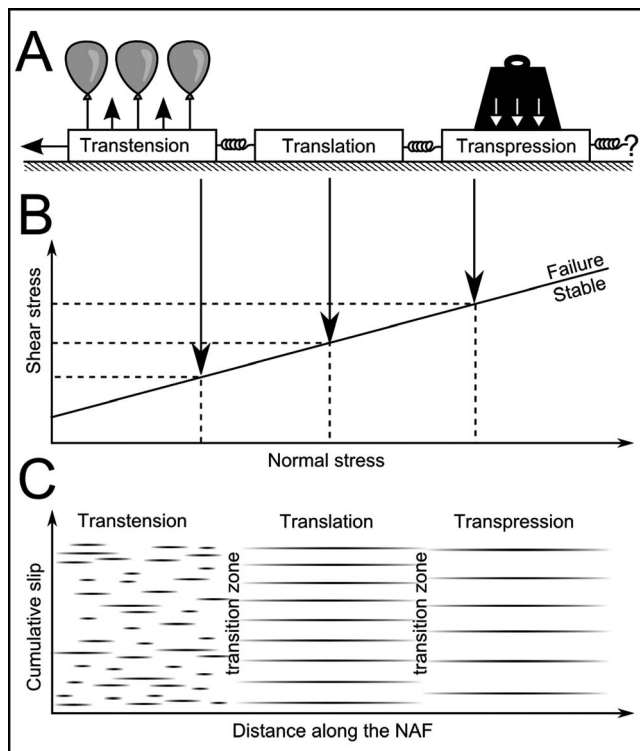


Figure 7. (a) Cartoon showing how blocks connected by springs being dragged along a surface, which is analogous to sections of a fault, can be modified to correspond to the sections of the NAF. (b) A schematic graph of shear stress versus normal stress showing a schematic stability field (which assumes that the strength of the fault is the same along the fault). Because of higher normal stress to the east along the NAF the amount of shear stress required to cause fault rupture is higher. (c) Schematic fault behavior diagram showing how the increase in fault-normal stress along the NAF might affect the spatiotemporal distribution of earthquakes. The furcation of the fault has been taken into account in the transtensional zone and the distribution of earthquakes is summed for all fault strands. The effect of the higher normal stress is to cause longer recurrence intervals.

which sections of the fault ruptured to cause this earthquake sequence. We have examined three scenarios (12, 12a, and 12b, Table 4) for the paleoearthquake PDFs that may fit with this earthquake. With the temporal resolution we presently have, it is not possible to attribute these paleoearthquake PDFs to the 1668 events alone i.e., there are other earthquakes in the historical record that are just as likely to have caused this fault rupture. Therefore, to truly understand this earthquake, more accurate dating techniques are required (better stratigraphic resolution, better choice of samples, or perhaps in combination with archaeoseismology).

[31] Because the 20th century earthquake sequence occurred in close succession (~ 60 years) and generally migrated from east to west, it is interesting to address the question: does the NAF always rupture in close succession? Because of the range in possible ages produced for each paleoearthquake (i.e., PDFs), it is difficult to make a specific

judgment. However, it does appear that sometimes large sections of the NAF rupture in close succession. For example, correlated paleoearthquake reference numbers (Table 4 and Figure 5) 15, 12, and 11 may correspond to a sequence of paleoearthquakes, but they are potentially spread over ~ 400 years. Along the 1943 and 1939 rupture segments (i.e., between ELM and CUK) the records are much longer and it appears that the paleoearthquakes on these segments are sometimes in phase, and sometimes out of phase. For example, correlated paleoearthquake reference numbers (Table 4 and Figure 5) 28 and 29, 36 and 37, 40 and 41, and 21, 19 and 20 may be in phase, whereas 33 and 34, 38 and 39, and 43 and 42 appear to be out of phase. Therefore, based on currently available paleoseismic data, the NAF may sometimes rupture in a migrating pattern, but possibly not as rapidly as the 20th century sequence, and probably not during every seismic cycle.

[32] There are many historical earthquakes (Table A1) that are not accounted for in the comparison with paleoearthquakes. Many of the unaccounted historical earthquakes are in the Sea of Marmara region, which are probably attributable to presently unstudied segments of the NAF. Others may have involved less active secondary faults associated with the plate boundary. It is also probable that some paleoearthquakes are simply not recognized at the paleoseismic investigation sites.

3.2.3. Comparison of Recurrence Intervals

[33] The summed interevent time (SIET) and average recurrence interval (RIavg) for each investigation are presented in Figure 6b and their 2σ ranges are summarized in Table 5. The RIavg and SIET have been summed along sections of the fault using a weighting based on the number of interevent times used to determine each one (Figures 6c and 6d, respectively). We consider the RIavg to provide a crude summary of the recurrence interval. By summing the RIavg for the three sections of the fault we observe five distinct peaks (Figure 6c). The peak corresponding to the longest interval is around 650–750 years and is due almost entirely to the paleoearthquake data from the 1939 rupture segment. A peak around 500 years is attributable to the results from the entire NAF. A peak around 400 years is attributable to the 1939 and 1943 rupture segments. Peaks around 100 and 300 years are attributable to the western section of the NAF. The key observations from the RIavg data are that the RIavg varies significantly between studies on the same section of the fault, and that the RIavg is generally shorter in the west than in the east.

[34] We consider the SIET to be more representative of the behavior of the fault as it accounts for the natural variability of interevent times, but also for all of the uncertainty associated with dating these paleoearthquakes. Therefore, the range of the SIETs is much longer. The range of SIETs is roughly 0–1000 years and is comparable to that of previously published estimates of recurrence interval (Table 1). We observe that there is a general agreement with the RIavg data, in that the recurrence interval is shorter in the west compared to the east. The key observations from the summed SIET data (Figure 6d) are that the western section and the 1939 rupture segment both show bimodal distributions, suggesting that there are two typical lengths of interevent time. In contrast, the 1943 rupture segment has a more normal distribution, suggesting that there is vari-

ability in the interevent time, but that it is usually a little less than 500 years.

[35] The variation in recurrence interval along the NAF suggests that it does not rupture in unison during every seismic cycle. The shorter recurrence intervals to the west and the bimodality of the western section and the 1939 rupture segments suggest that the fault behaves differently along strike.

4. Discussion

4.1. Fault Behavior

[36] Based on our analysis of the existing paleoseismic earthquake record it seems that the 20th century earthquake sequence that progressively migrated along the NAF is not typical of all seismic cycles on the NAF. In terms of fault behavior, we recognize three distinct sections along the NAF. The western-most ~600 km of the fault is typified by short paleoseismic records with a low number of paleo-earthquakes that, when analyzed, yield a relatively wide range in interevent times, which are distinctly shorter than the recurrence intervals of the fault sections to the east. The central section of the fault between ~600 km (Figure 2) and the Niksar pull-apart basin (~1050 km Figure 2) is typified by long paleoseismic records with generally corroborating paleoearthquake timing, suggesting that this section of the fault ruptures in unison or close succession. However, we note that there is a lack of data from the 1944 rupture segment. The eastern section, east of the Niksar pull-apart basin, is typified by long paleoseismic records, and the paleoearthquake PDFs suggest that during some seismic cycles, earthquakes only rupture part of the 1939 rupture segment. It is noted that more paleoseismic data are required from east of the Erzincan pull-apart basin to understand the behavior of the fault near the Karliova triple junction.

[37] The classification of the fault into these three sections is based on the paleoseismic data, but corresponds to tectonic provinces of Turkey [Şengör *et al.*, 1985] and sections of the fault described in section 2.1. Therefore, we suggest a correlation between varying fault behavior along the NAF and the tectonic provinces of the Anatolian plate. Figure 7 conceptually illustrates how the different tectonic regimes along the NAF affect the fault behavior in terms of Mohr-Coulomb failure criterion. This demonstrates how, as normal stress increases, the shear stress required to cause fault rupture also increases. Notably, we do not consider the implications of stress drop caused by fault rupture (i.e., under high normal stress the stress drop may be less). We do not attempt to quantify the stresses involved and recognize that each of the three main sections of the fault, particularly the western and eastern ends, are much more complex than indicated in Figure 7. It is also possible that the fault behavior is due to other characteristics of the tectonic provinces, e.g., crustal thickness.

[38] The western section is transtensional due to interaction of the west Anatolian extensional province with the right-lateral strike-slip of the NAF. The transtensional regime causes lower fault-normal stress that, according to Mohr-Coulomb failure criterion, means that less shear stress is required to cause fault rupture. Therefore, the low shear stress threshold causes smaller amounts of accumulated elastic strain to be released more frequently. Assuming that

the displacement rate is the same along the NAF, which is generally supported by geodetic observations [e.g., *Reilinger et al.*, 2006], this is a possible explanation for why there are more frequent earthquakes (i.e., short recurrence interval) along the western transtensional section of the NAF (as evidenced in the historical earthquake records, see Table A1). More frequent earthquakes mean that less strain accumulates between earthquakes and consequently the displacement per event is smaller in the west, relative to the east. Lower displacement per event and shorter rupture lengths, as a result of the fault furcation, mean that the earthquakes probably have relatively lower magnitude [*Wells and Coppersmith*, 1994]. As a consequence of the fault furcation, deformation and hence earthquake activity may switch between fault strands. Assuming the paleoseismic records are complete, we attribute the large variability in the SIET and RIavg on this western section of the NAF (Figure 4) to the short earthquake records (e.g., YGO and MST) and possibly switching between fault strands.

[39] The central translational section of the NAF has an intermediate fault-normal stress and a single dominant fault strand, except near its eastern end where the Ezinepazari fault ruptured to the south in 1939 (Figure 2) [*Barka*, 1996]. Therefore, this section of the fault relatively uniformly accommodates the westward translation of the Anatolian plate; hence the earthquake records along this section are relatively simple and generally correlate to each other. It is not entirely clear if the 1944 rupture segment is part of this section of the fault, because not enough studies on this section have been completed yet. As a consequence of the intermediate fault-normal stress and geometric simplicity of this section of the fault, it ruptures in unison or quick succession once enough shear stress has accumulated. The intermediate fault-normal stress and long rupture lengths may also help explain the relatively simple fault geometry. The simple fault geometry may also explain why long earthquake records have been determined in this area where the fault ruptures along the same strand repetitively. Despite the 1943 rupture section of the fault having relative temporal uniformity, there is evidence that the displacement per event is variable between seismic cycles [*Fraser et al.*, 2010; *Kozaci et al.*, 2007; *Sugai et al.*, 1999] (see section 2.6 for description of displacement per event). Together these two observations suggest that there is a weak or no relationship between accumulated strain and displacement per event on this section of the fault. However, more paleoseismic earthquake data, and displacement histories are required to substantiate this claim and to see if the 1944 rupture segment behaves in the same way.

[40] The eastern section of the NAF is transpressional due to the compressional fault-normal stress caused by the collision of Arabia into the southeastern side of the Anatolian plate. According to Mohr-Coulomb failure criterion, higher fault-normal stress requires a higher level of shear stress to cause fault rupture. Logically this would cause a longer recurrence interval between earthquakes. Figure 5 indicates that this is not the case for the last ~1000 years, but may have been prior to then. The younger age of some of the fault segments (e.g., the Kelkit valley segment was probably established when the Niksar pull-apart basin formed [*Fraser*, 2009]) may be associated with sections of higher frictional resistance on the fault plane, which, in conjunction

with the high fault-normal stress, may explain the relatively erratic behavior (i.e., sometimes the whole 1939 rupture segment ruptures, sometimes only part of it ruptures) of the eastern section of the NAF over the last ~1000 years. However, because there are multiple fault splays near the major pull-apart basins (e.g., Niksar and Erzincan basins [Barka *et al.*, 2000; Barka and Gülen, 1989]) and older basins along the fault (e.g., Suşehri and Gölova basins [Koçyiğit, 1989; Koçyiğit, 1990]), there may be some switching that leads to bimodal SIETs (e.g., sites RSA, GUN, and YAY).

[41] There are several possible causes of the bimodality of the SIETs observed at the eastern and western ends of the NAF. For example, parallel fault strands may accommodate some shear stress during some seismic cycles (switching [e.g., Dolan *et al.*, 2007]), stress triggering may significantly shorten some interevent times [e.g., Stein *et al.*, 1997], or leakage (i.e., a small amount of slip on one segment caused by rupture of an adjacent segment) may cause apparent variations in the interevent time at a point on the fault [e.g., Sieh, 1996]. Stress triggering may be caused by fault ruptures on adjacent segments of the NAF or other faults. For example, rupture of the eastern section of the NAF may be triggered by rupture of the East Anatolian, Ovacık or North East Anatolian faults. Now that we have described the significant influence of spatially variable fault-normal stress along the NAF, we speculate that the bimodality of the SIETs, observed predominantly on the eastern transpressional section (Figure 6), may be the result of time-varying fault-normal stress. Fluctuations in normal stress here may be related to spatiotemporal patterns of deformation on the East Anatolian and Dead Sea faults, or possibly from farther away (e.g., Red Sea, Gulf of Aden) [Migowski *et al.*, 2004]. For example, if the East Anatolian Fault ruptured along its full length in a sequence of events, it may change the fault-normal stress on the eastern section of the NAF, and hence this would change the shear stress failure threshold. We think that the bimodality observed in the summed SIETs for the western section of the NAF is attributable to switching between fault strands that accommodate different rates of deformation. However, longer earthquake records on the western section of the NAF may in the future reveal variation due to long-term changes in the fault-normal stress in the west Anatolian extensional province.

4.2. Future Work

[42] Future paleoseismic investigations on the NAF should focus on segments of the fault where studies have not yet been published, e.g., east of the Erzincan pull-apart basin, and in between existing studies. A relatively simple strategy to improve our understanding of how fault-normal stress affects the interevent time on the eastern transpressional section of the NAF would be to undertake similar compilation studies to this, perhaps along with more paleoseismic investigations, on the Dead Sea and East Anatolian faults and compare their results.

[43] We have recognized that studies that focus on one site for their investigation provide results that are more useful to this study, i.e., longer records with more dating. However, we do realize that not all studies target long accurate records of earthquake timing (e.g., some studies focus on displacement per event and slip rate). Furthermore,

the approach to using radiocarbon dates in paleoseismic investigations has evolved over the last 50 years, becoming progressively more concerned with quantifying uncertainty. Because incomplete reporting of the actual data in a particular study prevents their inclusion in compilations and future analyses it is desirable that future studies include the requisite information to ensure reproducibility.

[44] Stein *et al.* [1997] demonstrated that the 20th century earthquake sequence migrated along the NAF due to stress triggering. They recognized that one of the limitations of their model was that they used a common repeat and elapsed time for large earthquakes along the whole NAF. Perhaps the results of this study can be used to revisit such a model to investigate both the effect of stress triggering and try to model the behavior of the NAF in general.

5. Conclusions

[45] In this paper we explain how we have compiled a data set of all of the published paleoseismic data on the North Anatolian Fault (NAF). By selecting a subset of the data based on the length of the earthquake record, the precision of earthquake timing and the location of studies, we have investigated the spatiotemporal distribution of earthquakes. We compared the timing of earthquakes established in paleoseismic investigations along the NAF to each other and to the historical earthquake record. This exercise revealed that the 20th century earthquake sequence, which ruptured along almost the entire NAF, is not typical of the NAF, but may occur occasionally. The analyses suggest that the NAF does not rupture the same rupture segments during every seismic cycle, and that the NAF seems to behave differently within three distinct sections of the fault.

[46] The western-most section of the NAF (west of the where the NAF furcates) has relatively short earthquake records and a considerably shorter recurrence interval compared to farther east. We attribute this behavior to the interaction of the NAF with extensional stress associated with the west Anatolian extensional province [Şengör *et al.*, 1985], which ultimately reduces the shear stress required to cause fault rupture and promotes fault furcation. Therefore, this section of the NAF is transtensional and has shorter recurrence intervals.

[47] The central section of the NAF extends from where the fault furcates in the west to about the Niksar pull-apart basin in the east. This section of the fault shows the simplest behavior, appearing to predominantly rupture in quick succession or unison. Pending the results of investigations on the 1944 and 1942 rupture segments, it is presently unclear whether these rupture segments are part of this section of the fault. We attribute the behavior of the central segment of the NAF to the relative absence of tectonic fault-normal stresses; therefore, we call this the translational section of the fault.

[48] East of the Niksar pull-apart basin the paleoseismic record shows that the fault sometimes behaves like the central translational section of the fault with earthquakes, like the 1939 Erzincan earthquake, rupturing long sections of the NAF. However, sometimes it ruptures in shorter segments. We call this the transpressional section of the fault because of the probable high fault-normal stresses along this section of the fault associated with the east

Anatolian compressional province [*Şengör et al.*, 1985]. Based on the Mohr-Coulomb failure criterion, if this section of the fault is in transpression, then we should expect to see longer recurrence intervals. However, we see a prevalence of bimodal recurrence intervals, which suggests that sometimes the fault ruptures more frequently than others. This may be due to several causes, including interaction with other fault structures, or incomplete paleoearthquake records. However, we speculate that this may be caused by changes in the fault-normal stress due to seismic cycles on the East Anatolian and Dead Sea faults.

[49] The results of compiling the existing paleoseismic data from the NAF has led us to suggest that the pattern of fault ruptures over time is significantly influenced by fault-normal stress. Transtensional settings encourage short rupture lengths due to structural complexities and relatively low shear-stress failure thresholds. Translational areas, or those with little compression or extensional influence, promote faults that rupture in long segments, in close succession or in unison, and at moderate shear-stress thresholds. Transpressional settings promote variable fault rupture patterns over time, with long fault ruptures in unison or close succession during some seismic cycles and shorter rupture lengths during others. This compilation is a first step toward a better understanding of the long-term spatiotemporal behavior of the NAF, but it is clear that more paleoseismic data from the NAF and surrounding structures are required to substantiate the conclusions of this study.

Appendix A

[50] Table A1 provides a summary of the existing published historical earthquake information for earthquakes that have, or may have, ruptured the North Anatolian Fault. Because these data have come from a range of sources, there may be some events mentioned in historical literature that have been interpreted as different dates by the authors of the cited publications. We make no effort to resolve these discrepancies. It is difficult to accurately locate earthquakes and to establish if a surface rupturing earthquake occurred as this is seldom specified in the historical records. Furthermore, it is probable that some evidence for some earthquakes, are in fact evidence for more than one earthquake. For example, damage reported in two settlements hundreds of kilometers apart in a particular year may reflect one large fault rupture extending a great distance between the settlements, or two smaller earthquakes that occurred in the same year near each of the settlements that may or may not have involved any surface rupture. With little certainty on the extent of fault rupture and damage done by an earthquake, it is difficult to estimate the earthquake magnitude.

Appendix B: Review of Published Paleoseismic Investigations

[51] The results of paleoseismic studies vary significantly along the fault. Many investigations constrain the timing of one or two earthquakes and the temporal constraints on earthquakes vary considerably. This is a function of site selection, availability of dating materials, funding for field work and dating, and a component of luck. The luck component is generally a function of the unknown processes that

give rise to the deposits in a trench and their effect on the samples used for age constraint. Three key features of the paleoseismic investigations are used to decide whether or not they are included in the paleoearthquake model: number of paleoearthquakes identified, precision of paleoearthquake constraint, and the location of the investigation. A study that only identifies one or two paleoearthquakes is not very useful for this study. Studies that constrain the timing of paleoearthquakes to periods longer than about 500 years are not very useful either, because it is difficult to make comparisons of these data to the results from other studies and the historical earthquake record. Studies located in unique locations along the fault are more useful than studies in close proximity to each other.

[52] Sites are generally described from east to west. All data, including data we do not use in our analyses, are cataloged in Table S3 where the table structure shows all available data concerning dating samples and their stratigraphic position compared to the event horizons.

[53] At Kavakköy, trenching in 2001 by *Rockwell et al.* [2001] constrained the timing of five paleoearthquakes with the two youngest constrained in one temporal window. *Rockwell et al.* [2001] provided adequate data to allow us to determine unrounded calibrated radiocarbon ages. Four samples are shell material for which no reservoir correction (ΔR) was published so we include the rounded radiocarbon ages determined by in Table S3 but do not use these dates in our model. *Rockwell et al.* [2009] conducted a second study at this site and established the timing of four paleoearthquakes in individual temporal windows using a combination of selected radiocarbon dates from this and their 2001 study. Data from both studies at the Kavakköy site are used in the paleoearthquake model. Notably, the 2001 study has a low OxCal agreement index (Table 5), which we attribute to samples ^{14}C -14, 13, 3, and 33, which could be interpreted as reworked.

[54] *McHugh et al.* [2006] undertook a study of marine sediments at five locations in the Sea of Marmara using modern sampling and analysis techniques to identify the earthquake signature at each site. The data provided from the Ganos basin are too vague to incorporate in our model. Studies at Tekirdag basin, Central basin, and the Hersek Peninsula provide constraint on one, two, and two paleoearthquakes respectively. Although the temporal distribution of the paleoearthquakes suggests that they are incomplete records of the respective local earthquake chronology, these paleoearthquakes are included in the model because of their spatial uniqueness. We do not incorporate the study from the Gulf of İzmit because without further information we think it is not justifiable to date the event horizons with individual pieces of wood, as the age of the plant material is not clearly linked to earthquake occurrence. Most of the samples used by *McHugh et al.* [2006] are of a marine origin and therefore they use a reservoir correction (ΔR) of 81 ± 40 , which we have used with the “Marine_04” calibration curve [*Hughen et al.*, 2004].

[55] South of the Sea of Marmara, on the NAF between Yenice and Gönen, *Kürçer et al.* [2008] excavated three paleoseismic trenches. The central trench (Kar-1), near the village of Karaköy, was interpreted not to intersect the fault. The easternmost trench (Ket-1), near the village of Muratlar, identified the timing of the penultimate earthquake and

Table A1. Summary of Historical Earthquakes Which May Have Ruptured the NAF^a

Ref	Year	Magnitude	Name	Location	Ref (s) ^b	Epicenter	
						N°	E°
1	1999	Mw 7.1	Düzce	Adapazarı-Düzce-Bolu, the northern strand of the NAF locally ^c	1, 2	40.8	31.2
2	1999	Ms 7.4	İzmit (or Kocaeli)	Düzce, 30 km west of İzmit, the northern strand of the NAF locally ^c	1, 3, 2	40.64	29.83
3	1992	Ms 6.89	?	About 40 km east of Erzincan ^c	5, 6, 3	39.71	36.60
4	1967	Ms 6.1	?	East of Erzincan, south of Tercan	5, 6, 3	39.50	40.30
5	1967	Ms 7.21	Mudurnu	NAF surface rupture between Bolu and Geyve ^c	7, 5, 6, 3, 2, 4	40.70	30.70
6	1966	Ms 6.2	Varto	~150 km east, along the NAF, of Erzincan ^c	6	39.3	41.2
7	1966	Ms 6.85	Varto	~175 km east, along the NAF, of Erzincan	7, 5, 6, 3	39.20	41.40
8	1964	Ms 6.37	Manyas	Southern coast of the Sea of Marmara near Bandırma ^c	7, 6, 3, 2	40.07	28.95
9	1963	Ms 6.37	?	Near Istanbul on the north coast of the Sea of Marmara	7, 3	40.70	28.95
10	1959	MG 6	?	At the eastern end of the NAF north of Muş	7	39.1	41.6
11	1957	MG 6.25	?	Just north of the NAF ~30 km west of Bolu	7	40.7	31.2
12	1957	MG 6	?	Just north of the NAF ~30 km west of Bolu	7	40.7	31.2
13	1957	Ms 7.17	Abant	NAF surface rupture for ~50 km west of Bolu ^c	7, 5, 6, 3, 2, 4	40.60	31.00
14	1954	MG 6	?	North of the NAF near Samsun	7	41.1	36.3
15	1953	Ms 7.06	Gönen	On a strand south of the eastern Sea of Marmara ^c	7, 3, 6, 2	39.90	27.40
16	1951	Ms 6.92	Kurunlu	~40km rupture immediately east of Ilgaz ^c	7, 5, 6, 3	40.70	33.30
17	1949	Ms 6.87	?	On the NAF ~100 km east, along NAF, from Erzincan	7, 5, 6, 3	39.40	40.65
18	1944	Ms 6.83	Edremit	In the Aegean Sea near Edremit	7, 2, 3	39.70	26.50
19	1944	Ms 7.42	Bolu - Gerede	NAF surface rupture on the northern strand for 200 km east of Bolu ^c	7, 5, 6, 3, 4	41.05	32.20
20	1943	Ms 7.32	Tosya	End of 1942 rupture to Kurşunlu (~30 km northwest of Çankiri) ^c	7, 5, 6, 3, 4	41.00	33.50
21	1943	Ms 6.41	?	Northern strand of the NAF ~40 km east of İzmit	7, 6, 3	40.68	30.48
22	1942	Ms 7.12	Niksar-Erbaa	North side of the Niksar pull-apart ^c	7, 5, 6, 3, 4	40.70	36.40
23	1941	MG 6	?	On the NAF between Refahiye and Erzincan	7	39.8	39.3
24	1939	Ms 7.73	Erzincan	Just east of Erzincan to Niksar pull-apart and down the Ezinepazarı fault ^c	7, 8, 5, 6, 3, 4	39.70	39.70
25	1938	MG 6	?	North of Erzincan off of the NAF	7	39.9	39.7
26	1935	Ms 6.31	?	South of the eastern Sea of Marmara	7, 3	40.55	27.75
27	1935	Ms 6.41	?	South of the eastern Sea of Marmara	7, 3	40.50	27.60
28	1916	Ms 7.2	?	Between Niksar and Samsun - interestingly little evidence is known for this earthquake.	9	39.80	37.10
29	1912	Ms 6.8	Ganos	On the NAF on the Ganos Peninsula	3, 2	40.70	27.00
30	1912	Ms 7.4	Saros-Marmara	Ganos Peninsula (West of the Sea of Marmara) and western part of Sea of Marmara ^c	7, 8, 6, 2, 3, 10	40.70	27.20
31	1910	Ms 6.06	Osmancık	Near Osmancık ~20 km south of the main fault strand near Kargı	8, 3	40.88	34.56
32	1909	Ms 6.26	Endres	Off the NAF, ~25 km south of Koyulhisar, which is ~20 km west of Süşehri.	7, 8, 6, 3	40.17	37.76
33	1894	Ms 7.3	?	Near İzmit	2	40.7	29.6
34	1893	Ms 6.9	?	Near Enez at the northern end of the Aegean Sea, maybe not the NAF	2	40.5	26.2
34.5	1878	?	?	Locally destructive earthquake between Eşme, Sapanca and Adapazarı, with damage extending to Akyazı, İzmit and Bursa.	17	?	?
35	1866	Ms 7.2	Gonek	~140 km east of Erzincan along the northern EAF	6, 9	39.2	41.0
36	1859	Ms 6.8	?	In the Aegean Sea ~10 km off the Ganos peninsula, probably on the NAF	2	40.3	26.1
37	1855	Ms 6.6	Gemlik	~10 km south of Bursa	6	40.3	29.1
38	1855	Ms 7.1	Ulubat	~40 km west of Bursa, around Ulubat	6, 2	40.1	28.6
39	1794	Uk	?	Felt lightly in Istanbul reported from Bursa	11	?	?
40	1794	Uk	?	Major EQ reported in Çorum, Amasya, and Havza	11	?	?
41	1784	Ms 7.6	Elmalı	Affected the region from Erzincan to Muş, not clearly on the NAF	11, 6	39.5	40.2
42	1776	Uk	?	Near Merzifon which is 20 km SW of Havza also affected Amasya	11	?	?
43	1766	Ms 7.4	?	Western Sea of Marmara	11, 2	40.6	27.0
44	1766	Ms 7.1	?	Eastern Sea of Marmara	11, 2	40.8	29.0
45	1754	Uk	?	Possible EQ near Sivas, speculative	11	?	?
46	1754	Ms 6.8	?	Major damage to Istanbul caused by EQ in the Gulf of İzmit	11, 2	40.8	29.2
47	1752	Ms 6.8	?	Major damage in Edirne and villages to south of the Dardanelles	11, 2	41.5	26.7
48	1737	Ms 7	?	Damaging earthquake in the Biga region (South of the Sea of Marmara)	11, 2	40.0	27.0
49	1719	Ms 7.4	?	Eastern Sea of Marmara	11, 2	40.7	29.8
50	1684	Uk	?	Possibly an earthquake in northern Anatolia maybe near Niksar	11		
51	1672	Ms 7	?	80 km southwest of Çanakkale, near the eastern coast of the Aegean Sea	11, 2	39.5	26.0
52	1668	Ms 7.9	?	Reported in Ankara, Bolu, Konya, Ilgaz, Tokat, Havza, Amasya, Tosya	11, 6, 12	40.5	36.0

Table A1. (continued)

Ref	Year	Magnitude	Name	Location	Ref (s) ^b	Epicenter	
						N°	E°
53	1668	Uk	?	Large destructive EQ in Ankara	11	?	?
54	1668	Uk	?	Many shocks reported in Ankara- no evidence from other locations	11	?	?
55	1666	Uk	?	Unknown	11	?	?
56	1659	Uk	?	Reported damage to Erzurum (possibly 1660)	11	?	?
57	1659	Ms 7.2	?	~40 km north of Çanakkale in the eastern Aegean Sea	2	40.5	26.4
58	1648	Uk	?	Reported in Istanbul	11	?	?
59	1625	Ms 7.1	?	~40 km northwest of Çanakkale in the eastern Aegean Sea	2	40.3	26.0
60	1601	Uk	?	Damage to Erzincan and to the east	11	?	?
61	1598	Uk	?	Reported at Amasaya and the Black Sea coast (associated With reports of a tsunami)	11	?	?
62	1593	Uk	?	“Strong earthquake” reported in Istanbul	11	?	?
63	1590	Uk	?	Reported in Amasya	11	?	?
64	1583	Uk	?	Massive casualties reported from Erzincan	11	?	?
65	1579	Uk	?	Reported in Çorum, Amasya and Erzincan	11	?	?
66	1575	Uk	?	Reported in Erzincan	11	?	?
67	1567	Uk	?	Reported in Istanbul, İzmit and Sapanca	11	?	?
68	1556	Ms 7.1	?	Damage reported from all around the Sea of Marmara.	11, 2	40.6	28.0
69	1543	Uk	?	EQ reported in Çorum, Tokat and Erzincan	11	?	?
70	1535	Uk	?	Violent earthquake reported in Erzincan	11	?	?
71	1509	Ms 7.2	?	Sea of Marmara near Istanbul	11, 2	40.9	28.7
72	1500	Uk	?	EQ caused walls to collapse in Istanbul	11	?	?
73	1489	Uk	?	Possibly 1490, Istanbul	13	41.03	28.95
74	1481	Uk	?	Massive destruction of Erzincan 18k–32k deaths	13	39.73	39.50
75	1457	Uk	?	almost total destruction of Erzincan	13	39.73	39.50
76	1419	Ms 7.2	?	~35 km west of İzmit on the east coast of Sea of Marmara	6, 2, 13	40.4	29.3
77	1374	Uk	?	Erzincan city walls collapsed	13	39.73	39.50
78	1354	Ms 7.4	?	Ganos Peninsula, felt as far as Istanbul	2, 13	40.7	27.0
79	1344	Me 6	?	Eastern Sea of Marmara	13	40.68	27.40
80	1343	Ms 7	?	Istanbul	2, 13	40.9	28.0
81	1343	Ms 6.9	?	Istanbul	2, 13	40.7	27.1
82	1296	Ms 7.0	?	Istanbul	2, 13	40.5	30.5
83	1287	Uk	?	Erzincan (many victims)	13	39.73	39.50
84	1265	Uk	?	Sea of Marmara, reported on Marmara Island	13	40.63	27.62
85	1254	Ms 7.8	?	Near Refahiye, Suşehri (Reference 13 reports damage from Erzincan to Niksar)	6, 13	40.0	39.0
86	1237	Uk	?	Istanbul	13	41.03	28.95
87	1237	Uk	?	Strong earthquake in Erzincan (1236–1237)	13	39.73	39.50
88	1231	Uk	?	Istanbul	13	41.03	28.95
89	1206	Uk	?	Earthquake in Erzincan of unknown size (1206–1207)	13	39.73	39.50
90	1166	Uk	?	Erzincan, high numbers of fatalities (1165–1167)	13	39.73	39.50
91	1162	Uk	?	Istanbul	13	41.03	28.95
92	1143	Uk	?	Bursa	13	40.2	29.1
93	1090	Uk	?	Istanbul, significant damage	13	41.03	28.95
94	1065	Ms 6.8	?	Reported at İzmit (Nicaea)	2, 13	40.4	30.0
95	1063	Ms 7.4	?	Eastern edge of Ganos Peninsula	2, 13	40.8	27.4
96	1050	Ms 6.5	?	Çankırı ~10 km south of Ilgaz	6, 13	41.0	33.5
97	1045	Ms 7.5	?	Erzincan region, possibly south of Suşehri	6, 13	40.0	38.0
98	1043	Uk	?	This shock was associated with a region of ground ruptures from Erzurum to Nicopolis (Suşehri)	7	?	?
99	1035	Ms 6.5	?	~55 km west of Ilgaz (may correlate to the 1034–1035 earthquakes in reference 14)	6, 2, 13	40.8	33.0
100	1032	Uk	?	Istanbul	13	41.03	28.95
101	1026	Uk	?	Istanbul	13	41.03	28.95
102	1011	Uk	?	Erzincan	13	39.73	39.50
103	1010	Uk	?	Istanbul	13	41.03	28.95
104	989	Ms 7.2	?	Istanbul, İzmit (reference 14 gives date as 10/26)	14, 2	40.8	28.7
105	967	Ms 7.2	?	(Claudiopolis) ~10 km west of Bolu	14, 6, 2	40.7	31.5
106	869	Ms 7	?	Marmara, Istanbul	14, 2	40.8	29.0
107	860	Ms 6.8	?	Marmara, Istanbul (reference 14 place this earthquake at 862 5/28)	14, 2	40.8	28.5
108	824	Uk	?	Panion/Panium - eastern Sea of Marmara	14, 2	?	?
109	740	Ms 7.1	?	Reported broadly all around the Sea of Marmara	14, 2	40.7	27.7
110	557	Ms 6.9	?	Sea of Marmara	14, 2	40.9	28.3
111	554	Ms 6.9	?	Near İzmit, felt in Istanbul too (reference 14 gives date as 8/15)	14, 6, 2	40.7	29.8
112	543	Uk	?	Cyzicus (İzmit?)- Bandırma - southern Sea of Marmara	14	?	?
113	529	Uk	?	Amasia [sic] (Amasya)	14		
114	499	Ms 6.5	?	Earthquake destroyed Nicopolis, near Suşehri, also reported in the Niksar region	14, 6	40.5	37.0
115	484	Ms 7.2	?	On the northern side of the Ganos peninsula north of Gelibolu	2	40.5	26.6
116	478	Ms 7.3	?	Felt all around the Sea of Marmara (reference 14 477/480?)	14, 2	40.7	29.8

Table A1. (continued)

Ref	Year	Magnitude	Name	Location	Ref (s) ^b	Epicenter	
						N°	E°
117	460	Ms 6.9	?	Near Gönen (~5 km west)	14, 6, 2	40.1	27.6
118	447	Ms 7.2	?	Felt all around the Sea of Marmara	14, 2	40.7	30.3
119	442	Uk	?	Near Istanbul, could be small?	14	?	?
120	437	Ms 6.8	?	Near Istanbul	14, 2	40.8	28.5
121	407	Ms 6.8	?	Near Istanbul (could have been in 396)	14, 2	40.9	28.7
122	368	Ms 6.8	?	40 km east of Gönen, south of the Marmara Sea	2	40.1	27.8
123	368	Ms 6.8	?	Nicaea (İzmit)	14, 2	40.5	30.5
124	362	Ms 6.8	?	Nicaea (İzmit)	14, 2	40.7	30.2
125	358	Ms 7.4	?	İzmit	14, 2	40.7	30.2
126	368	Ms 7.3	?	Near İzmit on the eastern margin of the Sea of Marmara	6, 2	40.7	29.9
127	343	Uk	?	Niksar destroyed	14	?	?
128	269	Uk	?	(267–270) İzmit	14	?	?
129	236	Ms 6.5	?	Amasya region possibly near Lake Ladik	14, 6	40.9	36.0
130	181	Uk	?	İzmit	14	?	?
131	180	Ms 7.3	?	~55 km west of Bolu on the southern strand of the NAF	6, 2	40.6	30.6
132	160	Ms 7.1	?	~15 km southwest of Gönen- south of the Sea of Marmara	2	40.0	27.5
133	155	Ms 6.5	?	13 km west of Gönen (~Manyas?)	6	40.1	27.5
134	123	Ms 7	?	Southern coast of the Sea of Marmara, north of Gönen	2	40.3	27.7
135	121	Ms 7.4	?	İzmit destroyed (reference 14 dates to 120/128)	14, 2	40.5	30.1
136	69	Uk	?	Nicomedia (İzmit) possibly suffered an earthquake	14	?	?
137	68	Ms 7.2	?	Köseköy, eastern end of the Gulf of İzmit	2	40.7	30.0
138	32	Ms 7.2	?	~50 km southeast of İzmit on a southern strand of the NAF	6, 2	40.5	30.5
139	29	Uk	?	Nicaea (İzmit)	14	?	?
140	-287	Ms 7.5	?	Lysimachia was destroyed, - Ganos Peninsula	14	?	?
141	-360	Uk	?	Reported in Ophryneum, southwestern end of the Dardanelles (age approximate)	14	?	?
142	-427	Uk	?	Perinthus, northern coast of the Sea of Marmara south of Erdine	14	?	?
143	-1225 to -1175	Uk	?	It has been proposed that a sequence of earthquakes ruptured the NAF destroying many cities including the Hittite capital city of Hattusas over this period.	15, 16	?	?

^aEpicenter coordinates are in decimal degrees; in the “Magnitude” column, Uk is an abbreviation for unknown; years are shown as A.D., with negative indicating B.C. No interpretation has been applied to these historical data, please consult listed publications for further information.

^bReferences: 1, *Tibi et al.* [2001]; 2, *Ambraseys* [2002]; 3, *Ambraseys* [2001]; 4, *Barka* [1996]; 5, *Stein et al.* [1997]; 6, *Ambraseys and Jackson* [1998]; 7, *Ambraseys* [1970]; 8, *Ambraseys and Finkel* [1987]; 9, *Ambraseys* [1997]; 10, *Pondard et al.* [2007]; 11, *Ambraseys and Finkel* [1995]; 12, *Şengör et al.* [2005]; 13, *Guidoboni and Comastri* [2005]; 14, *Guidoboni et al.* [1994]; 15, *Nur and Cline* [2000]; 16, *Nur and Burgess* [2008]; 17, *Ambraseys and Finkel* [1991].

^cShown in Figure 2.

evidence of the 1953 Gönen earthquake. The westernmost trench (SEY-1), near the village of Seyvan, was interpreted to reflect three to four paleoearthquakes. We include these data, but do not use these data to constrain the poorly evidenced third and fourth events. We integrate the data from both trenches and recognize two events older than the 1953 Gönen earthquake (slightly different interpretation than the authors). The penultimate event is reflected in trench Sey-1 [*Kürçer et al.*, 2008, Figure 14] between units 1 and 2 due to three fault terminations at the base of unit 1 and the antepenultimate event is recognized between units 2 and 3 as unit 2 is clearly a colluvial wedge. *Kürçer et al.* [2008] published rounded conventional radiocarbon ages that we use in the paleoearthquake model.

[56] Very near the coastal town of Gölcük, *Klinger et al.* [2003] constrained the timing of two paleoearthquakes and clear geomorphic evidence of the 1999 İzmit earthquake. Both of these paleoearthquakes are incorporated into the paleoearthquake model. Because we use a Bayesian statistical model we must interpret the data that *Klinger et al.* [2003] published more critically because the model does not work if we input older ages over significantly younger ages, therefore we interpret 5 of the 14 ages northeast of the fault zone as being reworked (the two samples from the

southwest side of the fault are not demonstrably linked to the earthquake record). *Klinger et al.* [2003] published rounded conventional radiocarbon ages that are used in the paleoearthquake model.

[57] *Pavlidis et al.* [2006] undertook a trenching study involving five trenches at four sites (we are unsure of the exact locations) between Gölcük and Lake Sapanca. At the westernmost site, called D Deniz Evler, a trench was opened, which *Pavlidis et al.* [2006] interpret to have evidence for three, possibly four, paleoearthquakes including the 1999 İzmit earthquake. At the second site, Aşağı Yuvacık, a single paleoearthquake prior to the 1999 İzmit earthquake was identified. At the third site, Kullar Yaylacık, liquefaction features were recognized but no paleoearthquakes were constrained. At the eastern most site, Acisu, *Pavlidis et al.* [2006] identified three phases of sag pond development including a present-day sag pond, they claim to have identified a paleoearthquake in A.D. 1180 based on a single date but not enough evidence has been presented to convince us of this interpretation. *Pavlidis et al.* [2006] also describe a previously published trench at the Mahmutpaşa-çiftliği site although no earthquake timing data are presented. None of these studies are included in our paleoearthquake model because the temporal constraint on

earthquake timing is very vague or the record is very short. For example, at D niz Evler the second paleoearthquake is constrained between radiocarbon ages of 1080 ± 50 and 5580 ± 40 .

[58] Near K sek y, about 8 km east of the eastern tip of the Gulf of  zmit, *Rockwell et al.* [2001] determined that three paleoearthquakes occurred since the construction of an Ottoman canal. These data were used along with additional data by *Rockwell et al.* [2009] to constrain the timing of two paleoearthquakes and clear evidence of the 1999  zmit earthquake. Using the fraction modern carbon presented by *Rockwell et al.* [2009], we determine the unrounded conventional radiocarbon ages that are included in the paleoearthquake model. *Rockwell et al.* [2009] did not use an OxCal model for this site, we ran a model using all of the dates and found a very poor fit, which we attributed to the reworking of sample 6. By excluding this sample our model is consistent with the appropriately vague interpretation of historical earthquakes described by *Rockwell et al.* [2009].

[59] Approximately 20 km east of  zник, *Honkura and Isikara* [1991] undertook a trench near  erkeşli on the  zник–Mekece Fault, the southern strand of the NAF. They identified evidence for one paleoearthquake in their trench that they constrain to between 200 and 500 years BP. We have chosen not to include these data in our model as it is short and imprecise. About 30 km east of  erkeşli, *Yoshioka and Kuşcu* [1994] studied a site near Geyve also situated on the  zник–Mekece Fault. They found evidence for two paleoearthquakes, but these were only constrained by one radiocarbon date. Because this study defines one temporal window, over 2000 years long, containing evidence for two paleoearthquakes, these data are not included in the paleoearthquake model.

[60] *Ikeda et al.* [1991] and *Palyvos et al.* [2007] undertook paleoseismic investigations near one another in the Mudurnu Valley on the fault strand that ruptured in the 1967 Mudurnu valley earthquake. *Ikeda et al.* [1991] identified evidence for the 1967 Mudurnu valley earthquake and one older paleoearthquake, which their dating suggests occurred in the late second millennium A.D. Due to the poor constraint of their penultimate paleoearthquake and relatively short record we do not include these data in the paleoearthquake model. *Palyvos et al.* [2007] recognized evidence for the 1967 earthquake and constrained the timing of two additional earthquakes after approximately A.D. 1700. The one radiocarbon date used to constrain the maximum age of the two paleoearthquakes is modern, which means timing constraint of the paleoearthquakes is relatively poor. Because of the low number of paleoearthquakes, these data are not included in the paleoearthquake model.

[61] Four studies, involving multiple trench sites have been conducted in relatively close proximity on the D zce Fault that ruptured in the 1999 D zce earthquake [*Hitchcock et al.*, 2003; *Komut*, 2005; *Pantosti et al.*, 2008; *Pucci*, 2006; *Sugai et al.*, 2001]. *Sugai et al.* [2001] used a novel technique involving a geosclicer to constrain earthquake timing near Lake Efteni. *Sugai et al.* [2001] recognized evidence of the 1999 earthquake, two probable paleoearthquakes and two possible paleoearthquakes, which constitute an approximately 2000 year record. Because this paper is written in Japanese we are unsure exactly how the radiocarbon dating data have been processed and the strata

interpreted. *Sugai et al.* [2001, Table 1] provide conventional radiocarbon ages which are used in the paleoearthquake model. The interpretation of which samples are reworked is based on our interpretation of the geosclicer logs. Four sample ages of shell material are not used as no reservoir correction has been supplied and the ages they provide are discordant with the other ages from wood and soil. Of the remaining 16 samples, we interpret that three of them are reworked, and we do not use the two lowest samples as they are so old that they have no utility in our model.

[62] *Komut* [2005] claims to have constrained the timing of nine earthquakes using nine radiocarbon dates in five paleoseismic trenches on the D zce fault. We generally disagree with these interpretations and do not use data from this study from further discussion. Because the other studies on the D zce Fault [*Hitchcock et al.*, 2003; *Pantosti et al.*, 2008] comprise multiple trenches, at locations which overlap one another, Table S3 shows the data from each trench individually. We are unsure whether all of the dates are conventional radiocarbon ages; some are rounded while others are not. *Sugai et al.* [2001] provides us with a long earthquake record which is included in the paleoearthquake model. Because the studies of *Pantosti et al.* [2008] and *Hitchcock et al.* [2003] provide relatively short earthquake records and all of these studies are so close together, they are not included in the paleoearthquake model.

[63] East of their investigation on the D zce fault, *Hitchcock et al.* [2003] also opened test pits on the Bakack and Elmalik faults and established that they are active, but only at low levels, supporting the geometric evidence that suggests that these are linking structures between the D zce fault and the main strand of the NAF. Data from these studies are therefore not used in the paleoearthquake model.

[64] Near Gerede, two studies have been undertaken by *Kondo et al.* [2004] and *Okumura et al.* [2002, 2003]. These studies are the western-most studies east of the furcation of the NAF. *Kondo et al.* [2004] identified four paleoearthquakes including the 1944 Bolu–Gerede earthquake. These data are included in the paleoearthquake model using the published conventional radiocarbon ages. Twenty five samples were radiocarbon dated from the Demir Tepe site of which nine were interpreted as reworked. *Okumura et al.* [2002, 2003] identified six earthquakes at the Aridicli trench site, which is situated approximately 15 km east of the village of Gerede. We have not been able to locate the final results of this study so unfortunately it is not included in the paleoearthquake model.

[65] *Sugai et al.* [1999] undertook a paleoseismic investigation near Ilgaz in which they identified five paleoearthquakes including the 1943 Tosya earthquake (and possibly the 1944 Bolu–Gerede earthquake). This is a useful investigation but the publication does not state the radiocarbon ages or enough information to allow a critique of the quality of the investigation. Regrettably, this study is not included in the paleoearthquake model, however, because this study provides a long record in a unique location, we do consider the published earthquake ages (e.g., Figures 4 and 5).

[66] *Fraser et al.* [2010] undertook a paleoseismic investigation near Karalag ney at a site called Elmacik ~20 km northeast of Osmancık. The study determined the timing of seven earthquakes using a sequence of sediments deposited

against a fault scarp that were formed by a landscape response to intense ground shaking in a small steep catchment. Notably, this record is relict because there are no young sediments at the trench site, which is interpreted to reflect local stream incision that isolated the trench site from the sediment source. This study used an OxCal model which is included in the paleoearthquake model.

[67] Near Havza, *Yoshioka et al.* [2000] undertook an investigation that they interpreted to reveal the timing of two paleoearthquakes and the Tosya earthquake. We agree with the event horizons that *Yoshioka et al.* [2000] interpreted, but *Fraser et al.* [2010] identified another event horizon based on fault terminations in the published trench logs of *Yoshioka et al.* [2000], which we also use in the model. This study uses several bone fragments, and in some cases these radiocarbon ages may need a reservoir correction, but in this case the ages are conformable so no correction is applied. This study only published rounded conventional radiocarbon ages so these are used in the paleoearthquake model.

[68] Near Alayurt, approximately 10 km west of the western end of Lake Ladik, *Hartleb et al.* [2003] conducted a detailed trench study of a sag pond comprising two trenches. Their study constrained the timing of six earthquakes including the Tosya earthquake. Because they present only the rounded conventional radiocarbon age (“measured radiocarbon age”) we include these in the paleoearthquake model. In trench T1, *Hartleb et al.* [2003] documented four paleoearthquakes. They proposed two possible scenarios for their antepenultimate earthquake because of uncertainty concerning the origin of charcoal in a colluvial wedge deposit that may or may not have been reworked. Because it is not clear which of these scenarios is correct, we have created two separate models for Alayurt: Alayurt A assumes samples from unit 5 postdate the earthquake (the scenario preferred by the authors), and AlayurtB assumes samples from unit 5 predate the paleoearthquake. Like *Hartleb et al.* [2003], we consider that samples 123, 126, 127, 122, 105, 118, 104, and 115 are reworked. However, we did include sample 120, as it has the same age as sample 112 from the same stratigraphic unit. We also excluded the samples from their trench T3A from the OxCal model because of an excessive depositional hiatus in the strata. The T3A data constrain one additional paleoearthquake that is much older than any other known paleoearthquake on the NAF.

[69] About 6 km east of the eastern end of Lake Ladik, near Destek, *Fraser et al.* [2009] excavated a trench across a sediment trap formed by a transpressive splay of the NAF. Their study revealed the timing of 6–8 earthquakes including evidence of the 1943 Tosya earthquake. *Fraser et al.* [2009] used an OxCal model in their study so we use the same model in the paleoearthquake model.

[70] Just east of the Niksar basin, toward Reşadiye, *Fraser* [2009] conducted a paleoseismic investigation that defined the timing of six paleoearthquakes. This investigation was plagued by poor dating results and an anomalously large number of radiocarbon dates were excluded from the OxCal analysis by the authors. We incorporate the same OxCal model as presented by *Fraser* [2009] into the paleoearthquake model.

[71] *Zabci et al.* [2008] conducted six trenches at four locations between Reşadiye and Gölova in each of which

they encountered 2 or 3 paleoearthquakes. The results of these studies have only been tentatively described in conference proceedings and therefore the data required to include these studies in our model are not yet available.

[72] In the vicinity of Gölova, four paleoseismic studies have been undertaken by three different groups in relatively close proximity. Two investigations were conducted by *Zabci et al.* [2008]. *Okumura et al.* [1994b] undertook an exploratory trench study near Yukaritepecik (Suşehri site) however they have yet to publish their results. *Fraser* [2009] logged three paleoseismic trenches near the village of Günalan. Two of these trenches (T1 and T2) only identified 1 and 3 earthquakes with relatively poor accuracy compared to T3, the largest trench. Trench T3 revealed evidence of five paleoearthquakes and the 1939 Erzincan earthquake. The timing of the paleoearthquakes revealed in trench T3 was constrained using an OxCal model that we incorporate into the paleoearthquake model.

[73] About 30 km east of Gölova, toward the Erzincan pull-apart basin, two studies about 6 km apart have been conducted. The western study, at Yaylabeli [*Kozacı*, 2008], identified evidence for four paleoearthquakes and the 1939 Erzincan earthquake. The data from Yaylabeli has been included in our model. However, eleven of the thirty four dates that *Kozacı* [2008] used are the humic fraction of their samples. Radiocarbon samples are comprised of three fractions: (1) intact original carbon, the main constituent of the residual fraction, (2) degraded original organic carbon, and (3) contaminant carbon, fractions 2 and 3 comprise the humic fraction. We have excluded these samples from our analysis as these are duplicates of the residual fraction that include the contaminants and degraded carbon, hence they are less reliable. Of the remaining 23 samples, we interpreted five as being reworked (to get the OxCal file to work), which we also exclude from our model (three of these were also excluded in the OxCal analysis by *Kozacı* [2008]). It is noteworthy to mention that the OxCal agreement index (Table 5) for this study is very low relative to the other selected studies on the NAF, to a degree this is the result of having many event horizons in quick succession, therefore the paleoearthquake PDFs overlap with each other degrading the fit of the model. The results of this study are included in the paleoearthquake model.

[74] The eastern study, at Çukurçimen [*Hartleb et al.*, 2006], identified the timing of 6 paleoearthquakes including the Erzincan earthquake. We use the “measured radiocarbon age years BP” [*Hartleb et al.*, 2006, data repository item 2006140] which has been rounded and we assume is the conventional radiocarbon age. Although there is a sample age younger than the last earthquake, we drop this date and use the 1939 Erzincan earthquake as a boundary for the analysis. Out of the 42 radiocarbon ages that did not yield modern ages only two ages were reworked. These data are included in the paleoearthquake model.

[75] On the eastern side of the Erzincan pull-apart basin, *Okumura et al.* [1994a] conducted a paleoseismic investigation that revealed the timing of five paleoearthquakes. The paper about this investigation is predominantly written in Japanese so our interpretation relies primarily on interpretation of their figures. While we recognize that this increases the possibility of our misinterpretation, the long record and absence of other studies on this section of the fault have

encouraged us to utilize these data as best we can. We find it a little concerning that the errors on the radiocarbon ages are anomalously large compared to those from other studies, and it appears that these dates are a mixture of rounded and unrounded radiocarbon ages. Despite the confusion concerning the type of radiocarbon data, we incorporate this data into the paleoearthquake model. A total of 33 samples were dated, and we think that the authors are unsure of the location of seven of these samples, so we do not include these in the analysis. The top two samples are modern, so instead of including them in our model (the effect would be to spill some probability from a past earthquake into the future which is illogical) we use A.D. 1950 as a boundary for the model. Of the remaining 24 sample dates we interpreted four of them as reworked and five as contaminant.

[76] **Acknowledgments.** We acknowledge the European Commission for funding this project as part of the Marie Curie Excellence Grant Project "Understanding the irregularity of seismic cycles: A case study in Turkey" (MEXT-CT-2005-025617: Seismic Cycles). We would like to thank all of the authors who have published material that we have used from the NAF. Without their dedication to publish their results, this study would not be possible. Special thanks are given to Cecilia McHugh, Stefano Pucci, Tom Rockwell, Akin Kürçer, and Yann Klinger who all provided additional information about their studies on the NAF. We thank Caroline Ballard, George Hilley and an anonymous reviewer for constructive reviews of the manuscript.

References

- Akyüz, S. H., R. Hartleb, A. Barka, E. Altunel, G. Sunal, B. Meyer, and R. Armijo (2002), Surface rupture and slip distribution of the 12 November 1999 Düzce earthquake (M 7.1), North Anatolian Fault, Bolu, Turkey, *Bull. Seismol. Soc. Am.*, *92*(1), 61–66, doi:10.1785/0120000840.
- Allmendinger, R. W., R. Reilinger, and J. Loveless (2007), Strain and rotation rate from GPS in Tibet, Anatolia, and the Altiplano, *Tectonics*, *26*, TC3013, doi:10.1029/2006TC002030.
- Altunel, E., M. Meghraoui, H. Akyüz, and A. Dikbas (2004), Characteristics of the 1912 co-seismic rupture along the North Anatolian fault zone (Turkey): Implications for the expected Marmara earthquake, *Terra Nova*, *16*(4), 198–204, doi:10.1111/j.1365-3121.2004.00552.x.
- Ambraseys, N. N. (1970), Some characteristic features of the Anatolian fault zone, *Tectonophysics*, *9*, 143–165, doi:10.1016/0040-1951(70)90014-4.
- Ambraseys, N. N. (1997), The little-known earthquakes of 1866 and 1916 in Anatolia (Turkey), *J. Seismol.*, *1*(3), 289–299, doi:10.1023/A:1009788609074.
- Ambraseys, N. N. (2001), Reassessment of earthquakes, 1900–1999, in the eastern Mediterranean and the Middle East, *Geophys. J. Int.*, *145*(2), 471–485, doi:10.1046/j.0956-540x.2001.01396.x.
- Ambraseys, N. (2002), The seismic activity of the Marmara Sea region over the last 2000 years, *Bull. Seismol. Soc. Am.*, *92*(1), 1–18, doi:10.1785/0120000843.
- Ambraseys, N. N., and C. F. Finkel (1987), Seismicity of Turkey and neighboring regions, 1899–1915, *Ann. Geophys., Ser. B*, *5*(6), 701–725.
- Ambraseys, N. N., and C. F. Finkel (1991), Long-term seismicity of Istanbul and of the Marmara Sea region, *Terra Nova*, *3*(5), 527–539, doi:10.1111/j.1365-3121.1991.tb00188.x.
- Ambraseys, N. N., and C. F. Finkel (1995), *The Seismicity of Turkey and Adjacent Areas: A Historical Review, 1500–1800*, 240 pp., Muhittin Salih Eren, Istanbul.
- Ambraseys, N. N., and J. Jackson (1998), Faulting associated with historical and recent earthquakes in the eastern Mediterranean region, *Geophys. J. Int.*, *133*(2), 390–406, doi:10.1046/j.1365-246X.1998.00508.x.
- Armijo, R., B. Meyer, A. Hubert, and A. Barka (1999), Westward propagation of the North Anatolian Fault into the northern Aegean: Timing and kinematics, *Geology*, *27*(3), 267–270, doi:10.1130/0091-7613(1999)027<0267:WPOTNA>2.3.CO;2.
- Barka, A. A. (1992), The North Anatolian fault zone, *Ann. Tectonicae*, *6*, 164–195.
- Barka, A. (1996), Slip distribution along the North Anatolian Fault associated with the large earthquakes of the period 1939 to 1967, *Bull. Seismol. Soc. Am.*, *86*(5), 1238–1254.
- Barka, A. A., and L. Gülen (1989), Complex evolution of the Erzincan basin eastern Turkey, *J. Struct. Geol.*, *11*, 275–283, doi:10.1016/0191-8141(89)90067-9.
- Barka, A. A., and K. Kadinsky-Cade (1988), Strike-slip fault geometry in Turkey and its influence on earthquake activity, *Tectonics*, *7*(3), 663–684, doi:10.1029/TC007i003p00663.
- Barka, A. A., S. H. Akyüz, H. A. Cohen, and F. Watchorn (2000), Tectonic evolution of the Niksar and Tasova-Erbaa pull-apart basins, North Anatolian fault zone: Their significance for the motion of the Anatolian block, *Tectonophysics*, *322*, 243–264, doi:10.1016/S0040-1951(00)00099-8.
- Barka, A., et al. (2002), The surface rupture and slip distribution of the 17 August 1999 İzmit earthquake (M 7.4), North Anatolian Fault, *Bull. Seismol. Soc. Am.*, *92*(1), 43–60, doi:10.1785/0120000841.
- Bécel, A., et al. (2009), Moho, crustal architecture and deep deformation under the North Marmara Trough, from the SEISMARMARA Leg 1 offshore-onshore reflection–refraction survey, *Tectonophysics*, *467*, 1–21, doi:10.1016/j.tecto.2008.10.022.
- Biasi, G., and R. Weldon (1994), Quantitative refinement of calibrated C-14 distributions, *Quat. Res.*, *41*, 1–18, doi:10.1006/qres.1994.1001.
- Biasi, G. P., R. J. Weldon, T. E. Fumal, and G. G. Seitz (2002), Paleoseismic event dating and the conditional probability of large earthquakes on the southern San Andreas Fault, California, *Bull. Seismol. Soc. Am.*, *92*(7), 2761–2781, doi:10.1785/0120000605.
- Bronk Ramsey, C. (2007) *OxCal Program v. 4.0.5, Radiocarbon Accelerator unit*, Univ. of Oxford, Oxford, U. K. (Available at <https://c14.arch.ox.ac.uk/oxcal.html>)
- Cakir, Z., A. Akoglu, S. Belabbes, S. Ergintav, and M. Meghraoui (2005), Creeping along the North Anatolian Fault at Ismetpasa (western Turkey): Rate and extent from InSAR, *Earth Planet. Sci. Lett.*, *238*, 225–234, doi:10.1016/j.epsl.2005.06.044.
- Dolan, J., F. D. Bowman, and C. Sammis (2007), Long-range and long-term fault interactions in southern California, *Geology*, *35*(9), 855–858, doi:10.1130/G23789A.1.
- Flerit, F., R. Armijo, G. King, and B. Meyer (2004), The mechanical interaction between the propagating North Anatolian Fault and the back-arc extension in the Aegean, *Earth Planet. Sci. Lett.*, *224*(3–4), 347–362, doi:10.1016/j.epsl.2004.05.028.
- Fraser, J. G. (2009), Four new paleoseismic investigations on the North Anatolian Fault, Turkey, in the context of existing data, Ph.D. thesis, 284 pp., Univ. Libre de Bruxelles, Belgium, Brussels.
- Fraser, J. G., J. S. Pigati, A. Hubert-Ferrari, K. Vanneste, U. Avsar, and S. Altinok (2009), A 3000-year record of ground-rupture earthquakes along the central North Anatolian Fault near Lake Ladik, Turkey, *Bull. Seismol. Soc. Am.*, *99*(5), 2681–2703, doi:10.1785/0120080024.
- Fraser, J. G., A. Hubert-Ferrari, K. Vanneste, S. Altinok, and L. Drab (2010), A relict sedimentary record of seven earthquakes between 600 AD and 2000 BC on the central North Anatolian Fault at Elmacik, near Osmancik, Turkey, *Geol. Soc. Am. Bull.*, in press.
- Guidoboni, E., and A. Comastri (Eds.) (2005), *Catalogue of Earthquakes and Tsunamis in the Mediterranean Area From the 11th to the 15th Century*, 1037 pp., Ist. Naz. de Geophys. e Vulcanol., Bologna, Italy.
- Guidoboni, E., A. Comastri, and G. Traina (1994), *Catalogue of Ancient Earthquakes in the Mediterranean Area up to the 10th Century*, 504 pp., Ist. Naz. di Geofis., Rome.
- Hartleb, R. D., J. F. Dolan, H. S. Akyüz, and B. Yerli (2003), A 2000-year-long paleoseismologic record of earthquakes along the central North Anatolian Fault, from trenches at Alayurt, Turkey, *Bull. Seismol. Soc. Am.*, *93*(5), 1935–1954, doi:10.1785/0120010271.
- Hartleb, R. D., J. F. Dolan, Ö. Kozacı, H. S. Akyüz, and G. G. Seitz (2006), A 2500-yr-long paleoseismologic record of large, infrequent earthquakes on the North Anatolian Fault at Çukurçimen, Turkey, *Geol. Soc. Am. Bull.*, *118*(7), 823–840, doi:10.1130/B25838.1.
- Hilley, G. E., and J. J. Young (2008a), Deducing paleoearthquake timing and recurrence from paleoseismic data, Part I: Evaluation of New Bayesian Markov-Chain Monte Carlo simulation methods applied to excavations with continuous peat growth, *Bull. Seismol. Soc. Am.*, *98*(1), doi:10.1785/0120020077.
- Hilley, G. E., and J. J. Young (2008b), Deducing paleoearthquake timing and recurrence from paleoseismic data, Part II: Analysis of paleoseismic excavation data and earthquake behavior along the central and southern San Andreas Fault, *Bull. Seismol. Soc. Am.*, *98*(1) doi:10.1785/0120070012.
- Hitchcock, C., E. Altunel, A. Barka, J. Bachhuber, W. Lettis, and Ö. Kozacı (2003), Timing of late Holocene earthquakes on the eastern Düzce Fault and implications for slip transfer between the southern and northern strands of the North Anatolian fault system, Bolu, Turkey, *Turk. J. Earth Sci.*, *12*, 119–136.

- Honkura, Y., and A. M. Isikara (1991), Multidisciplinary research on fault activity in the western part of the North Anatolian fault zone, *Tectonophysics*, *193*, 347–357, doi:10.1016/0040-1951(91)90343-Q.
- Hubert-Ferrari, A., R. Armijo, G. King, B. Meyer, and A. Barka (2002), Morphology, displacement, and slip rates along the North Anatolian Fault, Turkey, *J. Geophys. Res.*, *107*(B10), 2235, doi:10.1029/2001JB000393.
- Hubert-Ferrari, A., G. King, J. Van der Woerd, I. Villa, E. Altunel, and E. Armijo (2009), Long-term evolution of the North Anatolian Fault: New constraints from its eastern termination, in *Collision and Collapse at the Africa–Arabia–Eurasia Subduction Zone*, edited by D. J. J. Van Hinsbergen et al., *Geol. Soc. Spec. Publ.*, *311*, 133–154, doi:10.1144/SP311.5.
- Hughen, K. A., et al. (2004), Marine04 marine radiocarbon age calibration, 026 cal kyr BP, *Radiocarbon*, *46*(3), 1059–1086.
- Ikeda, Y., Y. Suzuki, E. Herece, F. Şaroğlu, A. M. Isikara, and Y. Honkura (1991), Geological evidence for the last two faulting events on the North Anatolian fault zone in the Mudurnu Valley, western Turkey, *Tectonophysics*, *193*(4), 335–345, doi:10.1016/0040-1951(91)90342-P.
- Klinger, Y., K. Sieh, E. Altunel, A. Akoglu, A. Barka, T. Dawson, T. Gonzalez, A. Meltzner, and T. Rockwell (2003), Paleoseismic evidence of characteristic slip on the western segment of the North Anatolian Fault, Turkey, *Bull. Seismol. Soc. Am.*, *93*(6), 2317–2332, doi:10.1785/0120010270.
- Koçyiğit, A. (1989), Suşehri basin: An active fault-wedge basin on the North Anatolian fault zone, Turkey, *Tectonophysics*, *167*(1), 13–29, doi:10.1016/0040-1951(89)90291-6.
- Koçyiğit, A. (1990), Tectonic setting of the Gölova basin: Total offset of the North Anatolian fault zone, *E. Pontide, Turkey, Ann. Tectonicae*, *2*, 155–170.
- Komut, T. (2005), Paleoseismological studies on Düzce fault and geological data on the seismogenic sources in the vicinity of Düzce area, Ph.D. thesis, 155 pp., Boğaziçi Univ., Istanbul.
- Kondo, H., V. Özaksoy, C. Yildirim, Y. Awata, Ö. Emre, and K. Okumura (2004), 3D trenching survey at Demir Tepe site on the 1944 earthquake rupture, North Anatolian fault system, Turkey, in *Fourth Annual Publication of the Active Fault Research Center*, 231–242 pp., Geol. Surv. of Jpn., Tsukuba.
- Kondo, H., Y. Awata, Ö. Emre, A. Doğan, S. Özalp, F. Tokay, C. Yildirim, T. Yoshioka, and K. Okumura (2005), Slip distribution, fault geometry, and fault segmentation of the 1944 Bolu-Gerede earthquake rupture, North Anatolian Fault, Turkey, *Bull. Seismol. Soc. Am.*, *95*(4), 1234–1249, doi:10.1785/0120040194.
- Kozacı, Ö. (2008), Constancy of strain release rates along the North Anatolian Fault, Ph.D. thesis, 174 pp, Univ. of South. Calif., Los Angeles.
- Kozacı, Ö., J. F. Dolan, C. F. Finkel, and R. Hartleb (2007), Late Holocene slip rate for the North Anatolian Fault, Turkey, from cosmogenic ³⁶Cl geochronology: Implications for the constancy of fault loading and strain release rates, *Geology*, *35*(10), 867–870, doi:10.1130/G23187A.1.
- Kozacı, Ö., J. F. Dolan, and R. C. Finkel (2009), A late Holocene slip rate for the central North Anatolian Fault, at Tahtaköprü, Turkey, from cosmogenic ¹⁰Be geochronology: Implications for fault loading and strain release rates, *J. Geophys. Res.*, *114*, B01405, doi:10.1029/2008JB005760.
- Kürçer, A., A. Chatzipetros, S. Z. Tutkun, S. Pavlides, O. Ateş, and S. Valkaniotis (2008), The Yenice–Gönen active fault (NW Turkey): Active tectonics and palaeoseismology, *Tectonophysics*, *453*(1–4), 263–275, doi:10.1016/j.tecto.2007.07.010.
- Lettis, W., J. Bachhuber, R. Witter, C. Brankman, C. E. Randolph, A. Barka, W. D. Page, and A. Kaya (2002), Influence of releasing step-overs on surface fault rupture and fault segmentation: Examples from the 17 August 1999 İzmit earthquake on the North Anatolian Fault, Turkey, *Bull. Seismol. Soc. Am.*, *92*(1), 19–42, doi:10.1785/0120000808.
- Lienkaemper, J. J., and C. Bronk Ramsey (2009), OxCal: Versatile tool for developing paleoearthquake chronologies—A primer, *Seismol. Res. Lett.*, *80*(3), 431–434, doi:10.1785/gssrl.80.3.431.
- Mantovani, E., M. Viti, D. Babbucci, and D. Albarello (2007), Nubia-Eurasia kinematics: An alternative interpretation from Mediterranean and North Atlantic evidence, *Ann. Geophys.*, *50*, 341–366.
- McCalpin, J. (Ed.) (1996), *Paleoseismology*, 1 ed., 583 pp., Academic, San Diego, Calif.
- McHugh, C. M. G., L. Seeber, M. H. Cormier, J. Dutton, N. Cagatay, A. Polonia, W. B. F. Ryan, and N. Gorur (2006), Submarine earthquake geology along the North Anatolia Fault in the Marmara Sea, Turkey: A model for transform basin sedimentation, *Earth Planet. Sci. Lett.*, *248*(3–4), 661–684, doi:10.1016/j.epsl.2006.05.038.
- Migowski, C., A. Agnon, R. Bookman, J. Negendank, and M. Stein (2004), Recurrence pattern of Holocene earthquakes along the Dead Sea transform revealed by varve-counting and radiocarbon dating of lacustrine sediments, *Earth Planet. Sci. Lett.*, *222*(1), 301–314, doi:10.1016/j.epsl.2004.02.015.
- Nur, A., and D. Burgess (2008), *Apocalypse: Earthquakes, Archaeology, and the Wrath of God*, 309 pp., Princeton Univ. Press, Princeton, N. J.
- Nur, A., and E. H. Cline (2000), Poseidon's horses: Plate tectonics and earthquake storms in the Late Bronze Age Aegean and eastern Mediterranean, *J. Archaeol. Sci.*, *27*(1), 43–63, doi:10.1006/jasc.1999.0431.
- Okumura, K., T. Yoshioka, I. Kusçu, T. Nakamura, and Y. Suzuki (1994a), Recent surface faulting on the North Anatolian Fault east of Erzincan basin, Turkey. A trenching survey, *Summ. Res. Using AMS Nagoya Univ.*, *5*, pp. 32–48, Nagoya Univ., Nagoya.
- Okumura, K., T. Yoshioka, and I. Kusçu (1994b), Surface faulting on the North Anatolian Fault in these two millennia, in *Proceedings of the Workshop on Paleoseismology, U.S. Geol. Surv. Open File Rep.*, *94-568*, 143–144.
- Okumura, K., Y. Awata, T. Y. Duman, F. Tokay, I. Kuscu, and H. Kondo (2002), Rupture history of the 1944 Bolu-Gerede segment of the North Anatolian Fault: Gerede-Ardicli Trench re-excavated, *Eos Trans. AGU*, Fall Meet. Supp., Abstract S11B-1155.
- Okumura, K., T. K. Rockwell, T. Duman, F. Tokay, Y. Awata, H. Kondo, V. Ozaksoy and C. Yildirim (2003), Refined slip history of the North Anatolian Fault at Gerede on the 1944 rupture, *Eos Trans. AGU*, *84*(46), Fall Meet. Suppl., Abstract S12B-0384.
- Palyvos, N., D. Pantosti, C. Zabcı, and G. D'Addezio (2007), Paleoseismological evidence of recent earthquakes on the 1967 Mudurnu Valley earthquake segment of the North Anatolian fault zone, *Bull. Seismol. Soc. Am.*, *97*(5), 1646–1661, doi:10.1785/0120060049.
- Pantosti, D., S. Pucci, N. Palyvos, P. M. De Martini, G. D'Addezio, P. E. F. Collins, and C. Zabcı (2008), Paleoseismicity of the Düzce fault (North Anatolian fault zone): Insights for large surface faulting earthquake recurrence, *J. Geophys. Res.*, *113*, B01309, doi:10.1029/2006JB004679.
- Pavlides, S. B., A. Chatzipetros, Z. S. Tutkun, V. Özaksoy, and B. Doğan (2006), Evidence for late Holocene activity along the seismogenic fault of the 1999 İzmit earthquake, NW Turkey, in *Tectonic Development of the Eastern Mediterranean Region*, edited by A. H. F. Robertson and D. Mountrakis, *Geol. Soc. Spec. Publ.*, 635–647.
- Piper, J., O. Tatar, H. Gursoy, B. L. Mesci, F. Kocbulut, and B. Huang (2008), Post-collisional deformation of the Anatolides and motion of the Arabian indenter: A paleomagnetic analysis, *Earth Environ. Sci.*, *2*, 012011, doi:10.1088/1755-1307/1082/1081/012011.
- Pondard, N., R. Armijo, G. C. P. King, B. Meyer, and F. Flerit (2007), Fault interactions in the Sea of Marmara pull-apart (North Anatolian Fault): Earthquake clustering and propagating earthquake sequences, *Geophys. J. Int.*, *171*, 1185–1197, doi:10.1111/j.1365-246X.2007.03580.x.
- Pucci, S. (2006), The Düzce segment of the North Anatolian fault zone (Turkey): Understanding its seismogenic behavior through earthquake geology, tectonic geomorphology and paleoseismology, Ph.D. thesis, Univ. degli studi di Perugia, Perugia, Italy.
- Reilinger, R., et al. (2006), GPS constraints on continental deformation in the Africa–Arabia–Eurasia continental collision zone and implications for the dynamics of plate interactions, *J. Geophys. Res.*, *111*, B05411, doi:10.1029/2005JB004051.
- Reimer, P. J., et al. (2004), IntCal04 terrestrial radiocarbon age calibration, 0–26 ka cal BP, *Radiocarbon*, *46*(3), 1029–1058.
- Rockwell, T., A. Barka, T. Dawson, S. Akyuz, and K. Thorup (2001), Paleoseismology of the Gazikoy-Saros segment of the North Anatolia fault, northwestern Turkey: Comparison of the historical and paleoseismic records, implications of regional seismic hazard, and models of earthquake recurrence, *J. Seismol.*, *5*(3), 433–448, doi:10.1023/A:1011435927983.
- Rockwell, T., et al. (2009), Paleoseismology of the North Anatolian Fault near the Marmara Sea: Implications for fault segmentation and seismic hazard, in *Paleoseismology: Historical and Prehistorical Records of Earthquake Ground Effects for Seismic Hazard Assessment*, edited by K. Reicherter, A. M. Michetti, and P. G. Silva, *Geol. Soc. Spec. Publ.*, *316*(1), 31–54, doi:10.1144/SP316.3.
- Schwartz, D. P., and K. J.oppersmith (1984), Fault behavior and characteristic earthquakes; examples from the Wasatch and San Andreas fault zones, *J. Geophys. Res.*, *89*(B7), 5681–5698, doi:10.1029/JB089iB07p05681.
- Şengör, A. M. C., N. Görür, and F. Şaroğlu (1985), Strike-slip faulting and related basin formation in zones of tectonic escape: Turkey as a case study, in *Strike-Slip Deformation, Basin Formation, and Sedimentation*, edited by K. T. Biddle and N. Christie-Blick, *Soc. Econ. Paleontol. Mineral. Spec. Publ.*, *37*, 227–264.
- Şengör, A., O. Tüysüz, C. İmren, M. Sakaç, H. Eyidoğan, N. Görür, X. Le Pichon, and C. Rangin (2005), The North Anatolian Fault: A new look, *Annu. Rev. Earth Planet. Sci.*, *33*(1), 37–112, doi:10.1146/annurev.earth.32.101802.120415.
- Sieh, K. (1996), The repetition of large-earthquake ruptures, *Proc. Natl. Acad. Sci. U. S. A.*, *93*, 3764–3771, doi:10.1073/pnas.93.9.3764.

- Steier, P., and W. Rom (2000), The use of Bayesian statistics for ^{14}C dates of chronologically ordered samples: A critical analysis, *Radiocarbon*, 42(2), 183–198.
- Stein, R. S., A. A. Barka, and J. H. Dieterich (1997), Progressive failure on the North Anatolian Fault since 1939 by earthquake stress triggering, *Geophys. J. Int.*, 128(3), 594–604, doi:10.1111/j.1365-246X.1997.tb05321.x.
- Stuiver, M., and H. A. Polach (1977), Discussion: Reporting of ^{14}C data, *Radiocarbon*, 19(3), 355–363.
- Sugai, T., O. Emre, T. Duman, T. Yoshioka, and I. Kescu (1999), Geologic evidence for five large earthquakes on the North Anatolian Fault at Ilgaz, during the last 2000 years—A result of GSI-MTA international cooperative research, in *Proceedings of the Paleoseismology Workshop; March 15, 1999, Tsukuba, Japan*, edited by K. Satake and D. Schwartz, U.S. Geol. Surv. Open File Rep., 99-400, 66–72.
- Sugai, T., Y. Awata, S. Tooda, O. Emre, A. Dogan, S. Ozalp, T. Haraguchi, K. Takada, and M. Yamaguchi (2001), Paleoseismic investigation of the 1999 Duzce earthquake fault at Lake Efteni, North Anatolian fault system, Turkey, *Annual Report on Active Fault and Paleearthquake Researches*, 1, 339–351.
- Tibi, R., G. Bock, Y. Xia, M. Baumbach, H. Grosser, C. Milkereit, S. Karakisa, S. Zünbül, R. Kind, and J. Zschau (2001), Rupture process of the 1999 August 17 Izmit and November 12 Düzce (Turkey) earthquakes, *Geophys. J. Int.*, 144, F1–F7, doi:10.1046/j.1365-246x.2001.00360.x.
- Tirel, C., F. Gueydan, C. Tiberi, and J. P. Brun (2004), Aegean crustal thickness inferred from gravity inversion. Geodynamical implications, *Earth Planet. Sci. Lett.*, 228(3–4), 267–280, doi:10.1016/j.epsl.2004.10.023.
- Tutkun, Z., and S. Pavlides (2001), Small scale contractional-extensional structure and morphotectonics along the fault traces of Izmit (Turkey), *Bull. Geol. Soc. Greece*, 34(1), 345–352.
- Uysal, T. U., H. M. Mutlu, E. Altunel, V. Karabacak, and S. D. Golding (2006), Clay mineralogical and isotopic (K-Ar, $\delta^{18}\text{O}$, δD) constraints on the evolution of the North Anatolian fault zone, Turkey, *Earth Planet. Sci. Lett.*, 243, 181–194, doi:10.1016/j.epsl.2005.12.025.
- Wells, D. L., and K. J. Coppersmith (1994), New empirical relationships among magnitude, rupture length, rupture width, rupture area, and surface displacement, *Bull. Seismol. Soc. Am.*, 84(4), 974–1002.
- Wesnousky, S. G. (2006), Predicting the endpoints of earthquake ruptures, *Nature*, 444, 358–360, doi:10.1038/nature05275.
- Westaway, R. (2003), Kinematics of the Middle East and eastern Mediterranean updated, *Turk. J. Earth Sci.*, 12, 5–46.
- Yeats, R. S. (2007), Paleoseismology: Why can't earthquakes keep on schedule? *Geology*, 35(9), 863, doi:10.1130/focus092007.1.
- Yoshioka, T., and I. Kuşçu (1994), Late Holocene faulting events on the İznik-Mekece fault in the western part of the North Anatolian fault zone, Turkey, *Bull. Geol. Surv. Jpn.*, 45(11), 677–685.
- Yoshioka, T., K. Okumura, İ. Kuşçu, and Ö. Emre (2000), Recent surface faulting of the North Anatolian Fault along the 1943 Ladik earthquake ruptures, *Bulletin of the Geological Survey of Japan*, 51(1), 29–36.
- Zabci, C., V. Karabacak, T. Sancar, H. S. Akyuz, E. Altunel, H. GURSOY, and O. Tatar (2008), The possible eastward continuation of the 17 August 1668 Anatolian earthquake on the North Anatolian Fault (NAF), Turkey, *Geophys. Res. Abstr.*, 10, 05542.
- Zhu, L., B. Mitchell, N. Akyol, I. Cemen, and K. Kekovali (2005), Crustal thickness variations in the Aegean region and its implications for the extension of continental crust, *Eos Trans. AGU*, 86(52), Fall Meet. Suppl., Abstract T24C-06.
- Zor, E. (2008), Tomographic evidence of slab detachment beneath eastern Turkey and the Caucasus, *Geophys. J. Int.*, 175(3), 1273–1282, doi:10.1111/j.1365-246X.2008.03946.x.

J. Fraser, A. Hubert-Ferrari, and K. Vanneste, Seismology Section, Royal Observatory of Belgium, Av. Circulaire 3, B-1180 Brussels, Belgium. (jeph4e@gmail.com; aurelia.ferrari@oma.be; kris.vanneste@oma.be)